Rab18 and Rab43 have key roles in ER-Golgi trafficking

Selma Y. Dejgaard[1], Ayesha Murshid[1], Ayşegül Erman[1], Özge Kızılay[1], David Verbich[1], Robert Lodge[2], Kurt Dejgaard[3], Thi Bach Nga Ly-Hartig[4], Rainer Pepperkok[4], Jeremy C. Simpson[4,*] and John F. Presley[1,‡]

[1]Department of Anatomy and Cell Biology, McGill University, Montreal, Quebec, Canada, H3A 2B2
[2]Laboratoire d'Immunoretrovirologie, Centre de Recherche d'Infectiologie – CHUL, Quebec, Canada, G1V 4G2
[3]Department of Biochemistry, McGill University, Montreal, Quebec, Canada, H3G 1Y6
[4]Cell Biology and Biophysics Unit, EMBL, 69117 Heidelberg, Germany
*Present address: School of Biology and Environmental Science, UCD, Dublin, Ireland
‡Author for correspondence (e-mail: john.presley@mcgill.ca)

Accepted 19 May 2008
J. Cell Sci. 121, 2768-2781 Published by The Company of Biologists 2008
doi:10.1242/jcs.021808

Summary

Rabs and Arfs/Arls are Ras-related small GTPases of particular relevance to membrane trafficking. It is thought that these proteins regulate specific pathways through interactions with coat, motor, tether and SNARE proteins. We screened a comprehensive list of Arf/Arl/Rab proteins, previously identified on purified Golgi membranes by a proteomics approach (37 in total), for Golgi or intra-Golgi localization, dominant-negative and overexpression phenotypes. Further analysis of two of these proteins, Rab18 and Rab43, strongly indicated roles in ER-Golgi trafficking. Rab43-T32N redistributed Golgi elements to ER exit sites without blocking trafficking of the secretory marker VSVG-GFP from ER to cell surface. Wild-type Rab43 redistributes the p150^{Glued} subunit of dynactin, consistent with a specific role in regulating association of pre-Golgi intermediates with microtubules. Overexpression of wild-type GFP-Rab18 or incubation with any of three siRNAs directed against Rab18 severely disrupts the Golgi complex and reduces secretion of VSVG. Rab18 mutants specifically enhance retrograde Golgi-ER transport of the COPI-independent cargo β-1,4-galactosyltransferase (Galtase)-YFP but not the COPI-dependent cargo p58-YFP from the Golgi to ER in a photobleach assay. Rab18-S22N also potentiated brefeldin-A-induced ER-Golgi fusion. This study is the first comprehensive application of large-scale proteomics to the cell biology of small GTPases of the secretory pathway.

Supplementary material available online at
http://jcs.biologists.org/cgi/content/full/121/16/2768/DC1

Key words: ER-Golgi Trafficking, GFP, Golgi, Rab18, Rab43, Endoplasmic reticulum

Introduction

The primary organelles of the secretory pathway are the endoplasmic reticulum (ER) (Porter et al., 1945) and the Golgi complex (Golgi, 1898). The trafficking of membranes between major elements of the secretory pathway is largely mediated by discontinuous carriers (Palade, 1975). The specificity of trafficking pathways depends on the selective incorporation of cargo into newly forming transport intermediates, movement of these transport intermediates to the target membrane and subsequent recognition and fusion steps (Palade, 1975).

Virtually all of these steps are regulated by small Ras-family proteins in the Arf/Arl (Donaldson et al., 2005; Kahn et al., 2006) and Rab (Stenmark and Olkkonen, 2001; Zerial and McBride, 2001) subfamilies. Many Rabs are known to regulate distinct aspects of trafficking pathways, often by regulating tethers, SNARE (soluble NSF attachment receptor) proteins and motors (Zerial and McBride, 2001). For example, Rab5 binds to early endosome antigen 1 (EEA1) and forms a complex with SNARE proteins to mediate homotypic fusion of early endosomes (Christoforidis et al., 1999; McBride et al., 1999). Rab1 interacts with other tethers including p115 required for the fusion of pre-Golgi intermediates with Golgi membranes (Sztul and Lupashin, 2006). Rab6 regulates a microtubule/kinesin-dependent pathway originating at the trans-Golgi network (TGN) (Echard et al., 1998; Girod et al., 1999; White et al., 1999). Thus, many Rab proteins possess a characteristic organellar distribution and regulate a specific transport step (Chavrier et al., 1990; Zerial and McBride, 2001).

There are in excess of 60 Rab-family (Pereira-Leal and Seabra, 2001) and 29 Arf/Arl (Kahn et al., 2006) proteins in humans compared with 11 Rab/Ypt proteins (Lazar et al., 1997) and five Arf/Arls in yeast (Behnia et al., 2004; Huang et al., 1999). Studies in mammalian cells have provided evidence for organization of specific Rabs in 'Rab domains' (Sonnichsen et al., 2000), which possess distinct lipid compositions but may be defined in part also by Rab effector proteins capable of interacting simultaneously with different Rabs (De Renzis et al., 2002). Studies in yeast also find recruitment of Rabs to lipid domains and it has been proposed based on these data that lipids define in part the localization of Rab proteins (Sciorra et al., 2005). Arfs are found in pits coated with COPI (coat protein complex) or clathrin which may indicate the existence of other spatially delimited domains.

Because of their central roles, Arf/Arl and Rab proteins provide appealing initial starting points for molecular characterization of these trafficking pathways. The increased number of these proteins in mammals is believed primarily to derive from the larger number of trafficking pathways, particularly between the Golgi complex, cell surface and endosomes, in addition to the variety of cargo requiring transport. As a consequence, in more complex organisms, many Rab/Arf/Arl proteins would be expected to associate with the different

transport intermediates involved in post-Golgi trafficking. However, a smaller number of Arf/Arl/Rab proteins would be required to regulate trafficking between the ER and Golgi where many distinct protein-protein interactions are required (e.g. tethers, SNARE proteins and motors) on a small number of distinct transport intermediates.

To further investigate the molecular mechanisms of small GTPases on the Golgi complex, we identified and GFP-tagged the entire subset of Golgi-localized Ras-family GTPases (primarily Arf, Arl and Rab proteins). Of the poorly characterized proteins identified, four proteins (Arl6, Rab18, Rab30 and Rab43) showed clear localization to the Golgi and ER. Of these, all but Arl6 predominately localized to pre-TGN locations within the early secretory pathway. Further detailed characterization of two of these proteins (Rab18 and Rab43) yielded data consistent with roles in retrograde and anterograde Golgi-ER pathways, respectively.

Results

GFP-tagging and Golgi localization of Arf/Rab family candidate Golgi proteins

To determine the set of Golgi-associated Rab and Arf/Arl proteins, we compiled a list of Ras-family proteins identified from Golgi or COPI vesicle preparations (Gilchrist et al., 2006) by at least one unique peptide (see supplementary material Table S2). We additionally included Arl6 because a known Arl6-interacting protein Arl6IP2 (Ingley et al., 1999) was also identified. We expressed GFP fusions of each of these proteins in Vero cells, and stained with antibody against the Golgi marker GM130 and the nuclear stain DAPI (Fig. 1; see supplementary material Table S3).

ARFRP1, Arl6, Rab30 and Rab43 all gave a similar pattern of Golgi and ER staining in Vero cells (Fig. 1) and other cell lines including HeLa, NRK and COS7 (data not shown). We did not detect Golgi localization for Arl6-GFP in MDCK cells despite it showing consistent Golgi localization in the other cell lines (three or more independent experiments in each cell line). Rab18 consistently localized to an extended reticular structure resembling the ER and nuclear envelope in all transfected cell types examined, including HeLa, NRK, COS7 and Vero cells, while showing variable degrees of Golgi localization in Vero, COS7 and NRK cells.

Rab4 and Rab5 showed clear GFP labeling on the Golgi as well as punctae in Vero cells (see supplementary material Fig. S1), although not in NRK cells (data not shown). Of the poorly characterized proteins, only Rab35 was localized to numerous intracellular punctate structures resembling endosomes (Kouranti et al., 2006). However, it also showed strong cell surface localization (Fig. 1) and an absence of clear Golgi staining.

Rab24, identified by proteomic analysis on the ER but not on the Golgi (Gilchrist et al., 2006), stained the ER including nuclear envelope (data not shown) and not the Golgi. Arl1 and Rab10 showed diffuse staining, whereas Rab15 localized entirely to nuclei, possibly indicating failure of the GFP constructs to target. RabL3 localized to the cytoplasm and stress fibers (Fig. 1; and see supplementary material Fig. S2) but did not colocalize with β-tubulin (data not shown). However, 22 out of 35 GFP constructs localized at least partially to the Golgi (supplementary material Table S3), which correlated well with the results of the proteomic analysis.

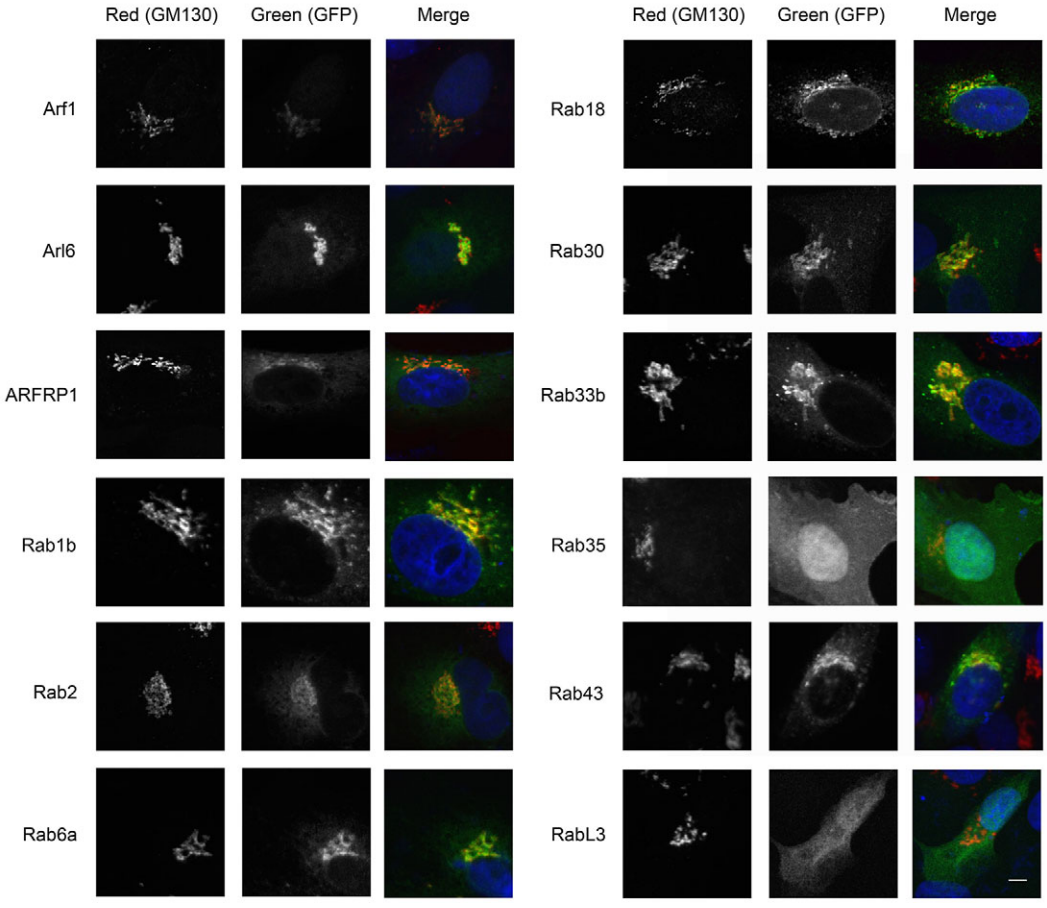

Fig. 1. Localization of GFP constructs. Vero cells on coverslips were transfected with the indicated GFP constructs and fixed 24 hours post transfection. Cells were subsequently stained with DAPI to visualize nuclei and antibodies against GM130 to visualize the Golgi complex. Scale bar: 5 μm.

Effects of mutations analogous to Ras dominant negatives on Golgi morphology

We next used overexpression assays to gain insight into possible roles of the Arl/Rab proteins in the secretory pathway. GFP-tagged wild-type and dominant-negative versions of all proteins were transfected into Vero cells (see supplementary material Table S3; Fig. 1 and Fig. 2A). Cells were subsequently immunostained for GM130 and DAPI to test for significant disruption of the Golgi complex, which was quantified by a measure of the Golgi area as described in Materials and Methods. By this measure, the strong dispersal of the Golgi complex produced by overexpression of Rab18 was unique among the tested wild-type constructs (Fig.

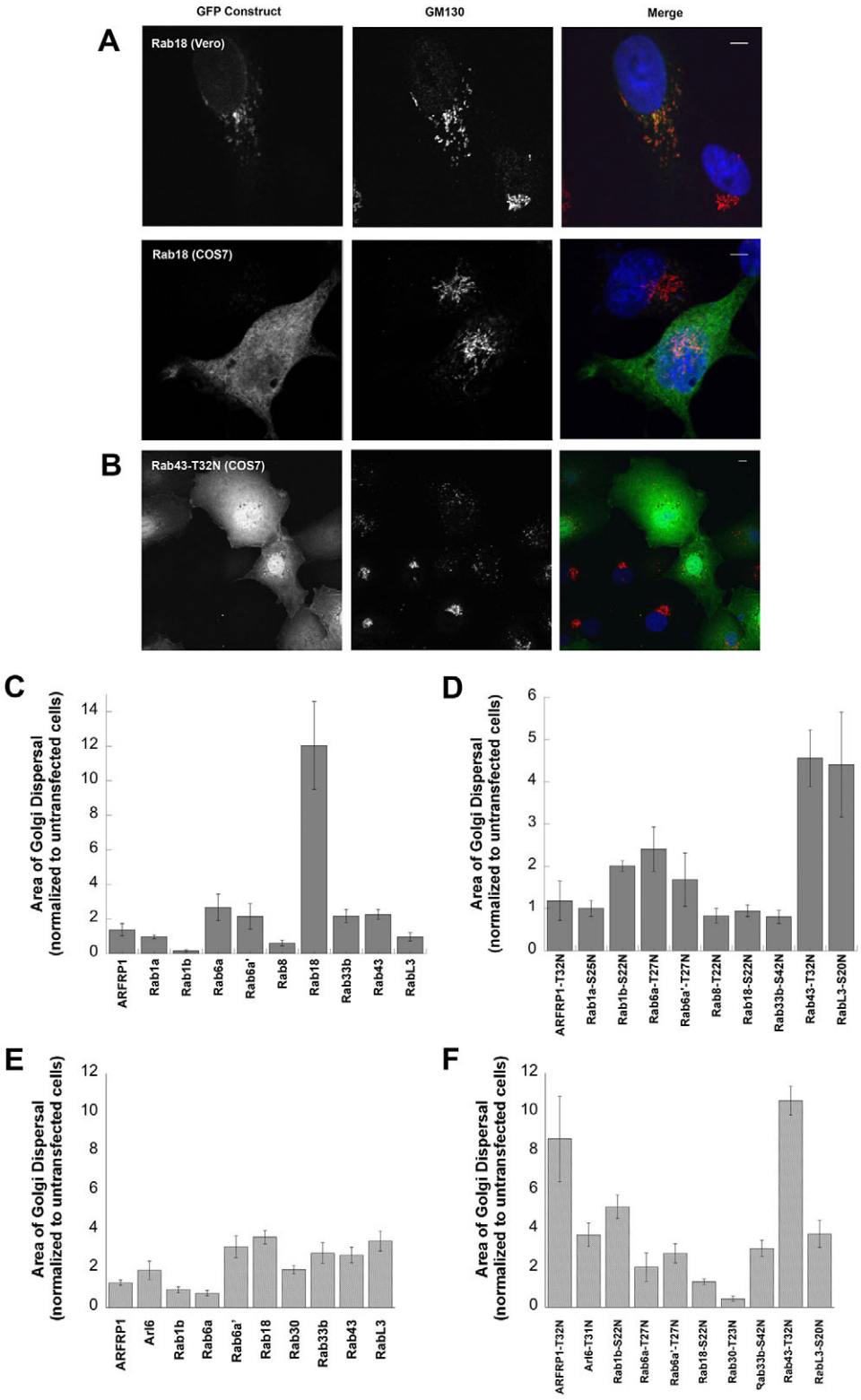

Fig. 2. Disruption of the Golgi complex by overexpression of dominant-negative or wild-type Rab proteins. Cells on coverslips were transfected with a panel of wild-type or dominant-negative GFP constructs. Coverslips were fixed 24 hours post transfection. GM130 staining was visualized by immunofluorescence using a Cy3-tagged secondary antibody. Nuclei were visualized using DAPI. (A) Dispersal of GM130 staining in Vero cells (top) and COS7 cells (bottom) expressing wild-type GFP-Rab18. (B) Dispersal of GM130 staining in multiple COS7 cells expressing dominant-negative Rab43. Scale bars: 5 μm. (C,D) Quantification of Golgi dispersal in Vero cells expressing the indicated wild-type Arl/Rab GFP constructs (C) or corresponding dominant-negative constructs (D). (E,F) Quantification of Golgi dispersal in COS7 cells expressing the indicated wild-type Arl/Rab GFP constructs (E) or corresponding dominant-negative constructs (F). Golgi dispersal was quantified and normalized to Golgi dispersal in untransfected cells on the same coverslip. Error bars indicate s.e.m.

2A,C). Overexpression of dominant-negative Rab43-T32N also produced a strong dispersal of the Golgi complex (Fig. 2D). However, Rab1b-S22N, a GDP-locked mutant of Rab1b, which has been previously shown to disrupt the secretory pathway when overexpressed (Plutner et al., 1991), produced only a twofold increase in dispersal of the Golgi complex (Fig. 2D). This is probably related to the lower expression levels in our Vero cells.

The quantitative measurement of Golgi dispersal was repeated in COS7 cells, because this cell line was able to support higher expression levels (Fig. 2E,F), resulting in a fivefold increase in Golgi dispersal for the positive control Rab1b-S22N (Fig. 2F). Under these conditions, overexpression of Rab43-T32N produced highly visible dispersal of Golgi staining with GM130-labeled punctae scattered throughout the cytoplasm (Fig. 2B) resulting in a tenfold increase in Golgi dispersal relative to untransfected cells (Fig. 2F). Dominant-negative ARFRP1-T32N also produced a large quantifiable effect in COS7 cells, but this appeared to be due to elongation of the Golgi complex in expressing cells, which in turn produced an exaggerated measure of Golgi scattering in our automated assay. Overexpression of wild-type Rab18 produced a milder visible phenotype in COS7 compared with Vero cells, but this equated to an almost fourfold increase in Golgi dispersal, which was greater than any other Rab protein tested including Rab6a and Rab33b, overexpression of which has been previously shown to disrupt Golgi morphology (Jiang and Storrie, 2005; Martinez et al., 1997; Valsdottir et al., 2001). Additional functional assays were also used to assess the importance of these Rabs. We measured the cell surface arrival of the temperature-sensitive vesicular stomatitis virus glycoprotein (ts-O45-G mutant) (VSVG) in cells overexpressing the wild-type Rab proteins, in an automated assay (Liebel et al., 2003) (supplementary material Fig. S4). The strongest retardation in secretion was observed in cells overexpressing Rab18, which is consistent with the effects seen on the Golgi complex upon overexpression of this protein.

In summary, overexpression of two proteins, Rab18 and Rab43-T32N, resulted in the dramatic redistribution of the Golgi protein GM130, with Rab18 also influencing the secretory capacity of cells, suggesting potential roles for these proteins in Golgi-ER trafficking.

Predominant localization of Rab/Arl proteins within the Golgi complex

The proteins identified could potentially regulate transport pathways between the ER and early (cis) Golgi or between late (trans) Golgi and post-Golgi compartments. We have recently developed a quantitative light microscopic assay that permits us to localize the major pool of transfected proteins to early or late Golgi regions (Dejgaard et al., 2007) (Fig. 3A,B). In this assay, Arl6 gave a clear trans Golgi localization (Fig. 3C). Rab18 presented particular difficulties as its predominant localization in NRK cells was to the ER. Nevertheless, in those cells where some Golgi localization of Rab18 was observed, it was the most cis-localized of all the proteins tested (Fig. 3C). Rab43 also gave a cis localization by this assay (Fig. 3C). Similar results were obtained in a fully automated version of this assay (Dejgaard et al., 2007) which required nocodazole treatment of cells to simplify Golgi geometry (see supplementary material Fig. S2B). Consistent results were obtained in a second cell line (HeLa) stained with GM130 (cis) and TGN46 (trans) using both the manual and automated methods (see supplementary material Fig. S3A,B). Efforts were taken to image cells expressing relatively low levels of GFP-proteins. However similar results were obtained across a range of expression levels.

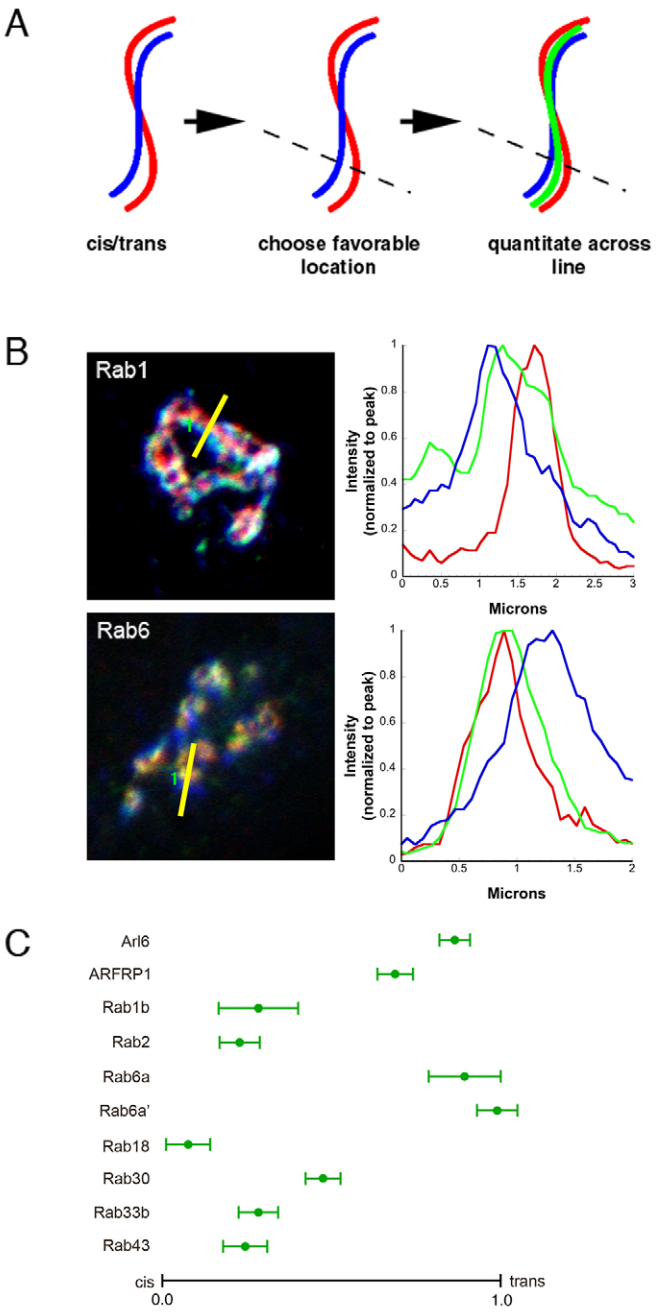

Fig. 3. Light microscopic localization of Rab proteins to Golgi subdomains. NRK cells were transfected with the indicated GFP constructs. 24 hours post transfection, cells were fixed and stained for p115 and TGN38. The cis-Golgi marker p115 was visualized using a Cy5-tagged secondary antibody (blue) and the trans-Golgi marker TGN38 was visualized using a Cy3-tagged secondary antibody (red). GFP constructs were scored for localization within the Golgi as described (Dejgaard et al., 2007). (A) Schematic illustrating choice of location for linescans. (B) Examples of linescans analyzed. (C) Mean location values determined for the indicated constructs. Mean values for 20 cells/sample are shown. Error bars indicate s.e.m.

Although this method has limited resolution compared to electron microscopy (e.g. closely apposed ER or intermediate compartment might not be distinguished from cis-Golgi) and transfected rather than endogenous proteins were examined, results with the control proteins (cis for Rabs 1 and 2, trans for 6a and 6a' and intermediate

for Rab33b) agreed closely with previous immuno-electron microscopic localizations. Rab18 and Rab43 clearly colocalized well with GM130, but only poorly with TGN38/46, consistent with the major pool of these proteins having an early Golgi localization. These proteins are thus excellent candidates for roles in ER/Golgi or intra-Golgi trafficking.

Arf/Rab proteins identified as Golgi associated are associated dynamically with the Golgi

Cytosolic Rabs are associated to GDP and require GTP exchange for recruitment to membranes, after which the Rab remains membrane-associated while GTP is bound. Rab proteins show very slow rates of spontaneous GTP hydrolysis, and must associate with GTPase activator proteins (GAPs) for efficient GTP hydrolysis. This is followed by rapid removal from membranes of Rab-GDP by Rab-GDI (Zerial and McBride, 2001).

A recent study identified a family of Rab-GAPs and suggested that only two Rab-GAPs (TBC1D20 and RN-tre), specific for Rabs 1, 2 and 43, are essential for Golgi function (Haas et al., 2007). To determine if other Rab/Arl proteins associated with Golgi membranes have a rapid association/dissociation cycle similar to Arf1 (Presley et al., 2002) and previously characterized Rab proteins (Vieira et al., 2003), suggesting interactions with Golgi GAPs and GEFs, we used a photobleaching approach (Presley et al., 2002). Analysis of recovery curves after photobleach of Golgi-associated proteins (Fig. 4) indicated all proteins tested, with the exception of ARFRP1, exchanged rapidly between the Golgi and cytosol with a $t_{1/2}$ for recovery of Golgi-associated fluorescence to a plateau value in the range of 60-120 seconds (Fig. 4B,C). This indicates functional interactions of Rab GAPs with multiple Rabs on the Golgi complex.

Effects of Rab43-T32N on Golgi morphology and secretory function

To further explore the importance of Rab43 function in the secretory pathway, we transfected COS7 cells with GFP-Rab43-T32N. In contrast to cells transfected with wild-type GFP-Rab43 (Fig. 1), the GM130 staining pattern was highly punctate. These punctate structures were immediately adjacent to ER exit sites (visualized with anti-COPII (Sec23 subunit) antibody; Fig. 5A) and contained Golgi markers including p115, COPI, ManII and TGN46 (data not shown).

To determine if the punctate elements identified in cells expressing GFP-Rab43-T32N were functional Golgi mini-stacks, we again examined the trafficking of the VSVG cargo tagged with CFP/YFP (Presley et al., 1997). COS7 cells grown on coverslips were doubly transfected with GFP-Rab43-T32N and with VSVG-CFP or singly transfected with VSVG-YFP and incubated for 24 hours at 40°C (non-permissive temperature) to accumulate VSVG-CFP in the ER. Cells were subsequently shifted to 32°C (permissive temperature to exit ER) for varying times. We found that in cells expressing GFP-Rab43-T32N, VSVG-CFP was largely accumulated on the cell surface at 3 hours (Fig. 5B). This was apparent in >90% of cells examined and at both low and high levels of Rab43-T32N expression. Thus, the secretory pathway was functional in cells expressing Rab43-T32N despite the dramatic changes in appearance of the Golgi complex.

A similar phenotype (scattering of the Golgi complex to ER exit sites but with preservation of secretory trafficking) is found in cells in which microtubules are destroyed by nocodazole (Cole et al., 1996) or in which interaction of pre-Golgi intermediates with the microtubule motor dynein/dynactin is blocked (Burkhardt et al., 1997). Examination of Golgi fragmentation induced by Rab1b-S22N and Rab43-T32N indicated that Rab43-T32N was effective at considerably lower expression levels (Fig. 5C). Since motors such as the dynein/dynactin complex are low abundance molecules, this could indicate a specialized role for Rab43 in recruiting microtubule motors. When a GFP-tagged version of the $p150^{Glued}$ subunit of dynein/dynactin (Watson and Stephens, 2006) was co-expressed with CFP-Rab43, which did not redistribute the Golgi markers examined, $p150^{Glued}$ lost its microtubule localization and became largely cytosolic (Fig. 5D,E). These results taken together suggest a potential role for Rab43 in regulation of anterograde trafficking from ER to Golgi.

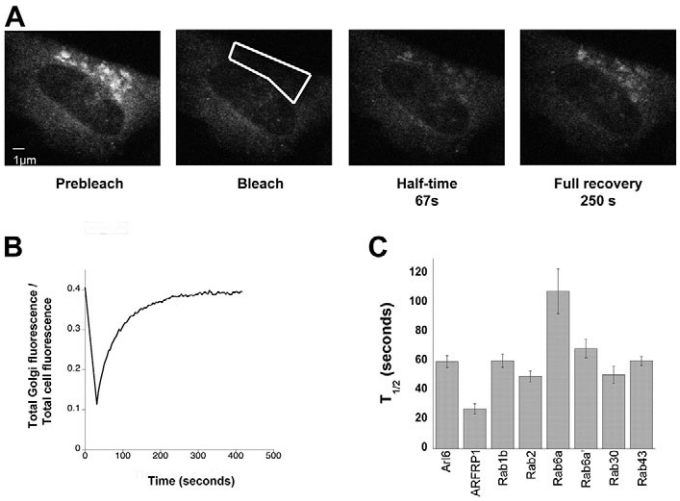

Fig. 4. Dynamics of Golgi association of GFP constructs. NRK cells in glass-bottomed dishes were transfected with the indicated GFP constructs and time-lapse sequences taken 24 hours post transfection. (A) Frames from a typical time-lapse sequence from a NRK cell expressing GFP-Rab43 showing a prebleach image with typical Golgi and cytoplasmic labeling, ablation of Golgi fluorescence by photobleach and points in the recovery time sequence. (B) Recovery curve from cell shown in A. Golgi fluorescence as proportion of total cell fluorescence is plotted. (C) Mean half-times (seconds) for the indicated proteins. Error bars indicate s.e.m.

Effects of overexpression or inhibition of Rab18 on the Golgi-ER system

Previous studies have indicated that Rab18 can localize to lipid droplets under certain circumstances (e.g. Martin et al., 2005; Ozeki et al., 2005) and to endosomes (Lutcke et al., 1994). We were able to confirm that GFP-Rab18 partially localized to lipid droplets induced by oleic acid treatment in Vero cells (see supplementary material Fig. S5) and in HeLa cells (data not shown) although a major pool of GFP-Rab18 did not appear to be localized to lipid droplets (see supplementary material Fig. S5). Others (Martin et al., 2005) have also noted consistent localization of Rab18 to the ER, even after induction of lipid droplet formation.

To further explore the disruption of the Golgi complex caused by Rab18 overexpression, we examined the distribution of various other markers. We found that COPI, ManII and p115 colocalized with GM130 punctae, (data not shown). An activated mutant of Rab18 (Q67L) analogous to a GTPase-defective mutant of Ras (Feig and Cooper, 1988) gave a similar phenotype of scattering GM130 staining (data not shown). GM130 staining was often scattered to

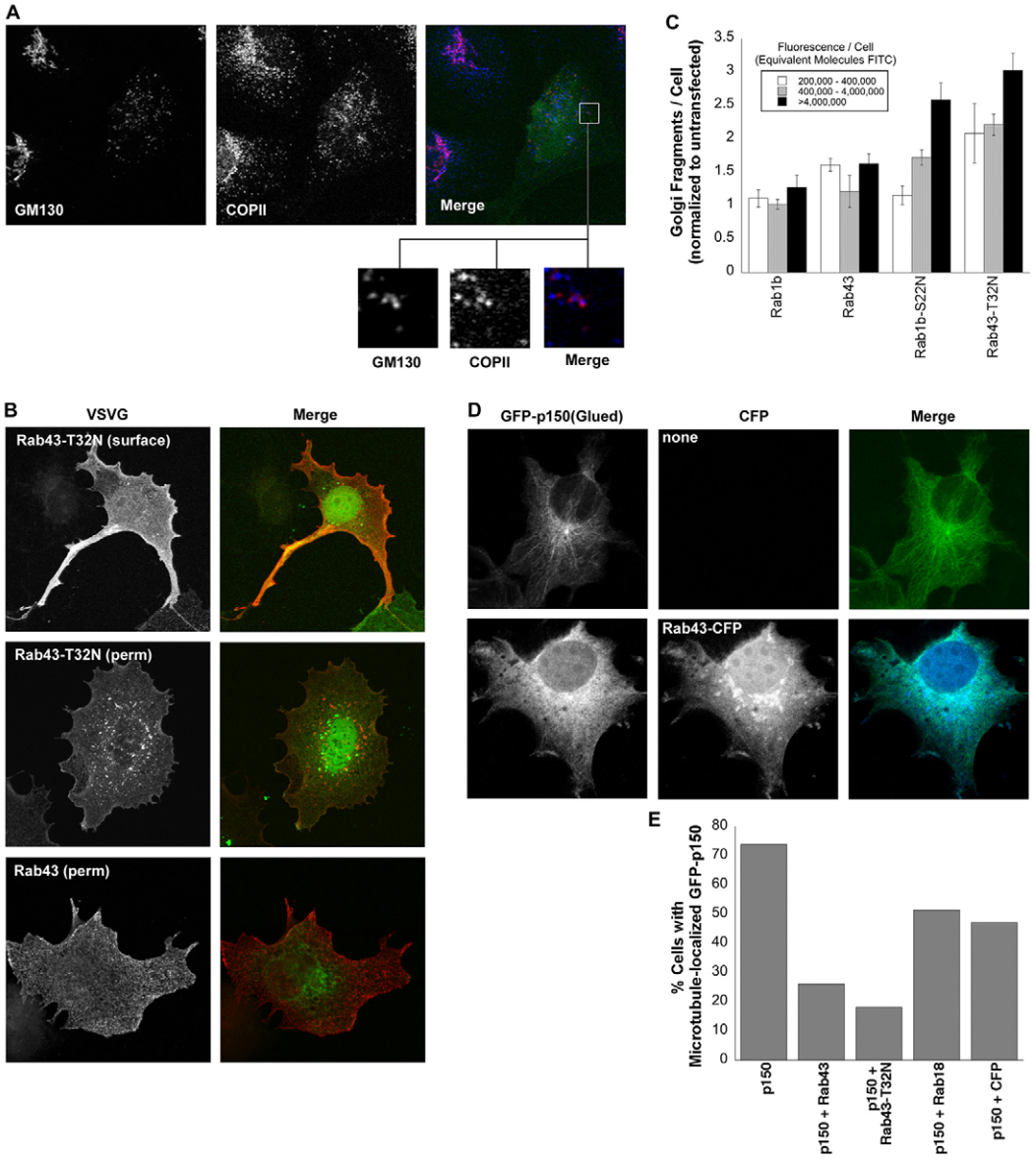

Fig. 5. The Golgi complex is functional but relocated to ER exit sites in COS7 cells expressing Rab43-T32N. (A) Colocalization of GM130 (Cy3; red) with COPII (Cy5; blue) in cell expressing GFP-Rab43-T32N (24 hours post transfection). (B) VSVG-CFP transport to the cell surface in cells expressing GFP-Rab43-T32N (top, middle) or GFP-Rab43 (bottom). Cells were stained without permeabilization to visualize surface VSVG-CFP (Cy3; red) or with permeabilization to visualize total VSVG-CFP as indicated. (C) Total Golgi fragments in cells expressing the indicated GFP-Rab construct. Cells were transfected with the indicated GFP-Rab constructs and were fixed and stained 24 hours post transfection. Transfected cells were divided into three expression levels based on GFP fluorescence and Golgi fragments were counted. Data are mean ± s.e.m. (D) Dispersal of GFP-p150^{Glued} from microtubules in cells expressing CFP-Rab43 (bottom). (E) Scoring of GFP-p150^{Glued} localization to microtubules in singly transfected cells or cells transfected with CFP-Rab43, CFP-Rab43-T32N, Rab18 or Clontech CFP N1 vector. 100 cells were scored for each condition.

COPII positive punctae, suggesting relocalization of Golgi components to ER exit sites with high expression levels of Rab18 constructs (Fig. 6B) comparing to low expression levels (Fig. 6A) of this protein.

We had found that overexpression of GFP-Rab18 for 24 hours in a standardized screen using HeLa cells resulted in a reduction in VSVG trafficking to the cell surface (supplementary material Fig. S4), indicating a potential role for Rab18 in secretion. We conducted additional experiments, co-transfecting COS7 cells on coverslips with CFP-Rab18 and with VSVG-YFP. Coverslips were kept at 40° C for 48 hours after transfection to ensure high expression levels of Rab18 constructs followed by shifting to 32°C. In cells singly transfected with VSVG-YFP or in cells from double-transfected coverslips but lacking CFP-Rab18 fluorescence, staining with the VG antibody was readily visible on the surface of non-permeabilized cells (Fig. 6C). However, in non-permeabilized cells expressing CFP-Rab18 (Fig. 6D), or CFP-Rab18-Q67L (not shown) little or no VG staining was detected. This was confirmed by quantitative analysis (see Materials and Methods) of the fraction of total VG on the cell surface (Fig. 6F). Thus, CFP-Rab18 but not CFP-Rab18-S22N or a negative control (CFP-Rab5) blocks VSVG trafficking to the cell surface (Fig. 6F) The lesser inhibition by Rab18-S22N was surprising but as CFP/YFP Rab18-S22N shows some membrane association, one explanation is that it has residual GTP exchange activity and thus acts as a weakly active wild-type rather than a dominant negative. There was little effect of GFP-Rab18 expression (48 hours) on uptake of the endocytic markers transferrin or EGF (Fig. 6G), indicating that effects of Rab18 overexpression were specific to the secretory pathway. At shorter Rab18 expression times (24 hours) the block in VSVG trafficking was only partial, consistent with a dose-dependent overexpression effect (data not shown), similar to the results obtained in HeLa cells after 24-hour expression (supplementary material Fig. S4).

We next examined Golgi morphology and secretion of VSVG in cells depleted for Rab 18 with three independent siRNAs found to reduce the levels of the Rab18 mRNA by 60 – 94% (depending on the siRNA; Fig. 7A). We found that the siRNA giving the best knockdown (94%; siRab18-1) reduced VSVG secretion by 60%

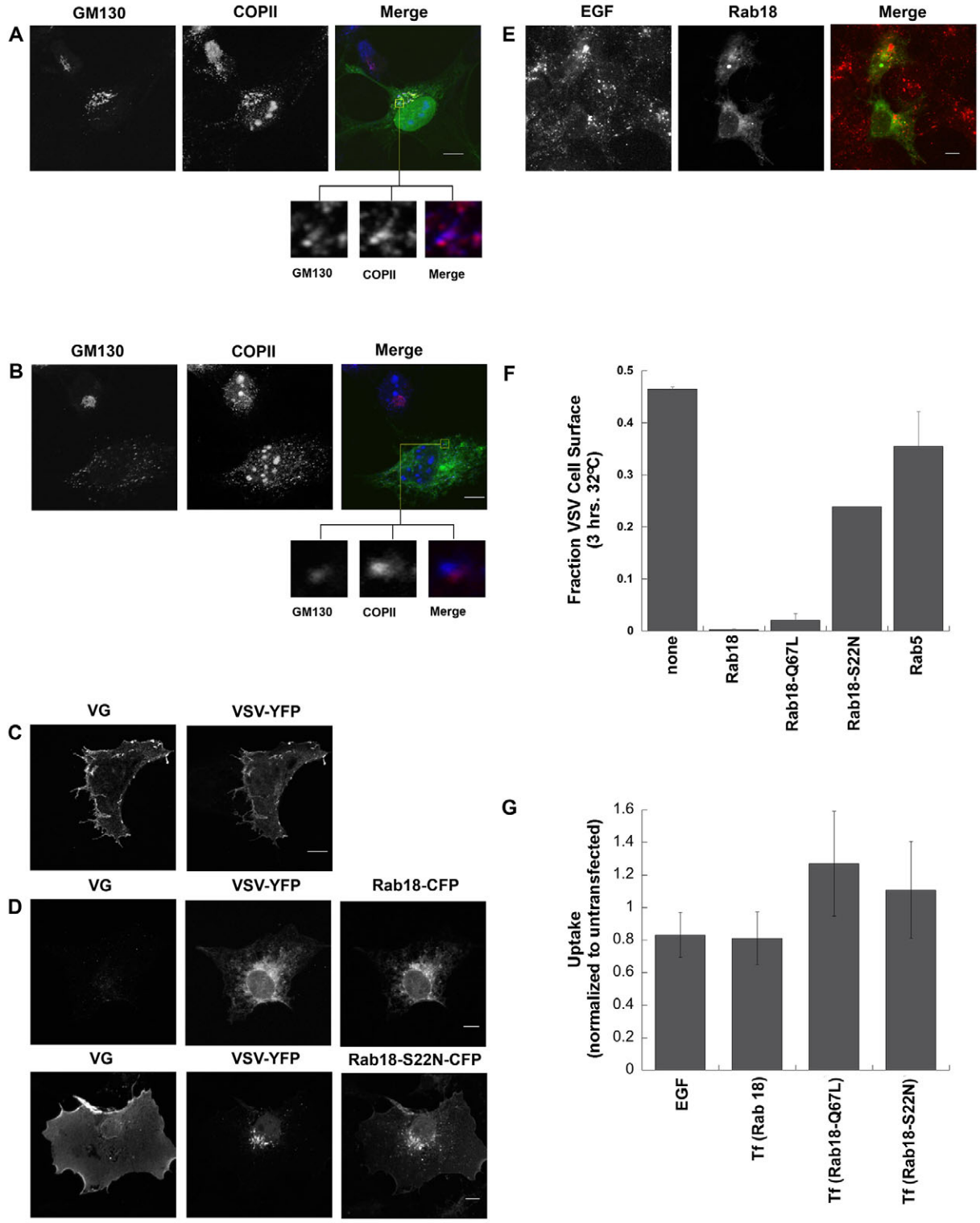

Fig. 6. Effects of overexpression of Rab18 in COS7 cells. (A) Colocalization of GM130 and COPII in immunofluorescence images of cells expressing moderate levels of GFP-Rab18. GM130 was visualized using a Cy3-tagged secondary antibody (red), COPII using Cy5 (blue). (B) Colocalization of GM130 and COPII staining in cells overexpressing very high levels of GFP-Rab18 staining was as in A. Magnifications of boxed areas are shown below merged images in A and B. (C,D) Trafficking of VSVG in cells strongly expressing Rab18 then incubated at 40°C for 48 hours to accumulate VSVG-YFP in the ER. Cells were then fixed and stained with VG antibody without permeabilization to detect cell-surface VSVG. (C) Singly transfected cells (VSVG-YFP only) were incubated at 32°C for 3 hours to allow exit from the ER. (D) Cells double-transfected with VSVG-YFP and the indicated Rab18 construct after shifting to 32°C for 3 hours. (E) Uptake of Cy3-EGF (100 ng/ml; for 30 minutes following a 2 hour serum starvation) in COS7 cells expressing GFP-Rab18 for 48 hours. Scale bars: 10 μm. (F) Quantification of the VSVG trafficking experiment in D. Each measurement is an average of >100 cells. (G) Quantification of endocytosis of Cy3-Tf (25 μg/ml; for 30 minutes following 2 hours of serum starvation) or EGF in cells expressing the indicated constructs for 48 hours. >100 cells were averaged for each sample. Data are mean ± s.e.m.

(Fig. 7B) and produced readily visible Golgi fragmentation with a six-fold increase in the total number of Golgi fragments detectable by light microscopy (Fig. 7C). This Golgi fragmentation was in excess of that produced by an siRNA directed against Rab1A (Fig. 7), which is well known to be required for secretory pathway function. Similar, albeit less pronounced, effects were produced by two independent siRNAs directed against Rab18, corresponding to the observation that these oligonucleotides showed a relatively lower reduction in the levels of Rab18 mRNA, as judged by RT-qPCR analysis (60-65% knockdown) (Fig. 7A). Golgi structure is normally maintained by interactions with the ER via trafficking pathways (Cole et al., 1996), thus disruption of the Golgi by either overexpression or down-regulation of Rab18 suggests a possible role for Rab18 in regulation of ER/Golgi trafficking.

Overexpression of Rab18 mutants enhances retrograde trafficking

To determine the effect of Rab18 and its mutants on cycling between the Golgi and ER (Zaal et al., 1999), we doubly transfected COS7 cells on glass-bottomed dishes with Galtase-YFP and with CFP-Rab18 or CFP-Rab18-S22N. The COPI-independent cargo Galtase-YFP has been localized to late Golgi compartments (Zaal et al., 1999) and its cycling between the Golgi and ER has been quantitated in HeLa cells using a photobleach assay (Zaal et al., 1999). COS7 cells singly transfected with Galtase-YFP were used as controls. Confocal image sequences were taken in which the Golgi was photobleached after acquisition of an initial prebleach image (Fig. 8A) as previously described (Presley, 2005).

In control cells, fluorescence was distributed between the Golgi complex and a dispersed pool which has been shown to be the ER (Zaal et al., 1999) (Fig. 8A). After photobleaching, Golgi fluorescence recovered on a timescale of 20-40 minutes (Fig. 8A). Recovery curves fit well to an inverted exponential with little or no immobile fraction (Fig. 8C). Thus, trafficking of Galtase-YFP between the ER and Golgi was considered to follow first order kinetics for analysis purposes. An ER-to-Golgi rate constant (k_{in}) and Golgi-to-ER rate constant (k_{out}) were calculated (see Materials and Methods, Fig. 8E).

Similar analysis was performed in cells double-transfected with Galtase-YFP and CFP-Rab18 or CFP-Rab18-S22N. Prebleach (i.e. steady-state) ratio of Golgi to non-Golgi fluorescence, ranged from roughly 70% Golgi/30% non-Golgi for control cells to 30% Golgi70% non-Golgi for cells expressing CFP-Rab18-S22N. Recovery curves could be fitted well to inverted exponentials with little immobile fraction as in controls. Golgi residence time ($1/k_{out}$) was 22.8 minutes for Galtase-YFP in singly transfected cells (Fig. 8F). This was faster than the Golgi residence time of 57.2 minutes measured previously in HeLa cells by similar methods (Zaal et al., 1999). An ER residence time ($1/k_{in}$) of 11.6 minutes was calculated for control cells (Fig. 8G).

Coexpression of Galtase-YFP with CFP-Rab18 for 48 hours led to a sharp reduction in both Golgi and ER residence times (to roughly 2 minutes each; Fig. 8F,G). These rates are too fast to explain by typical membrane trafficking pathways and are most compatible with the structures being Golgi remnants partly continuous with the ER [similar to 'BFA bodies' (Orci et al., 1993)] rather than true Golgi. Diffusion of Galtase-YFP between connected membranes could occur on the timescale of this experiment. Such severe disruption of the secretory pathway would be consistent with the fact that VSVG trafficking to the cell surface is efficiently blocked under the same conditions (Fig. 6C,D).

Overexpression of CFP-Rab18-S22N reduced but did not completely block trafficking of VSVG-YFP, indicating the presence of functional Golgi complex. We repeated the Galtase-YFP cycling assay in cells co-transfected with CFP-Rab18-S22N in an attempt to identify selective effects on trafficking pathways. In co-transfected cells, there was a modest reduction in Galtase-YFP ER residence time from 11.6 minutes to 8.4 minutes (Fig. 8G). In contrast, Golgi residence times were reduced seven-fold from 22.8 minutes to 3.3 minutes (Fig. 8F). These results are most consistent with a massive selective enhancement of a Golgi-to-ER retrograde trafficking pathway in cells expressing CFP-Rab18-S22N.

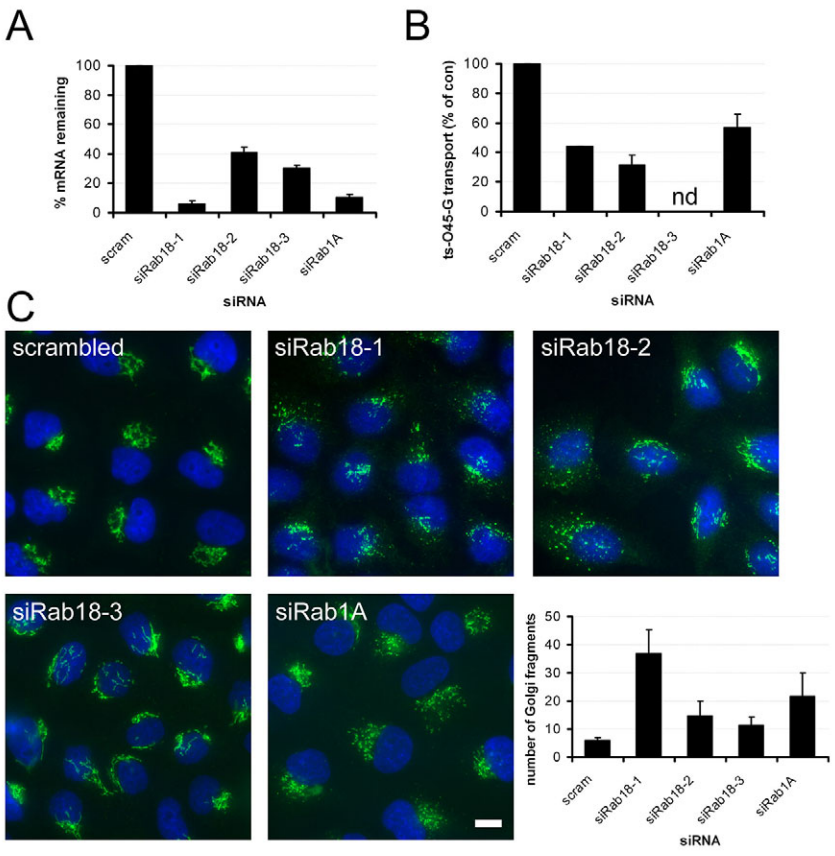

Fig. 7. Effect of siRNAs against Rab18 in HeLa cells. HeLa cells were incubated for 50 hours with either nonsilencing siRNAs (scrambled) or siRNAs targeting Rab18 or Rab1A, as indicated. (A) RT-qPCR determination of remaining mRNA in cells after treatment with the various siRNAs. (B) Quantification of relative cell surface arrival of VSVG (ts-O45-G) (Simpson et al., 2007) in cells treated with various siRNAs. (C) Examination of Golgi morphology, as judged by immunostaining of GM130, in cells incubated with various siRNAs. Quantitative determination of the number of detectable Golgi fragments in these cells as described (Liebel et al., 2003) is shown in the lower right graph. Scale bar: 10 μm. Error bars in graphs show the s.d. between three replicate experiments.

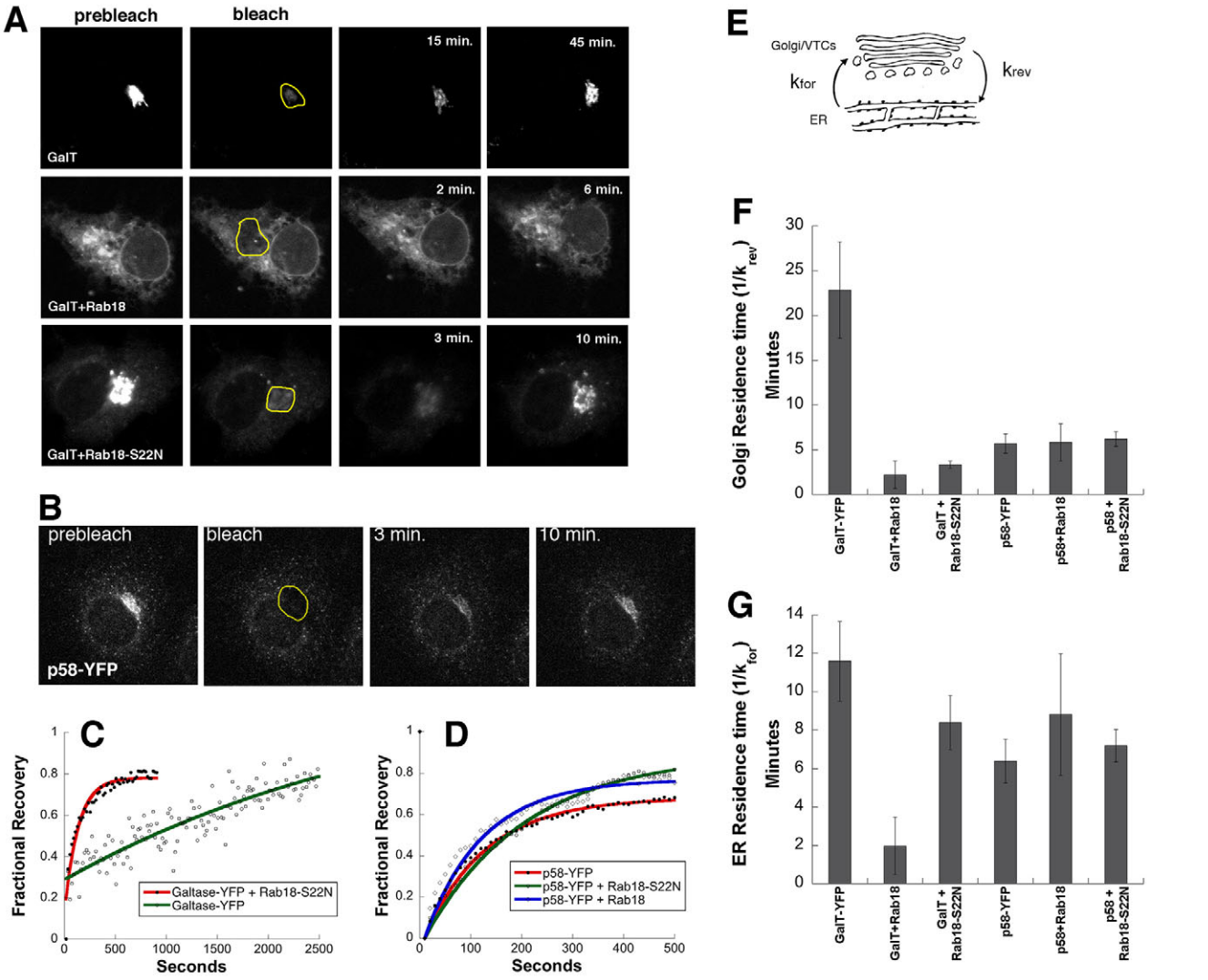

Fig. 8. Influence of Rab18 and Rab18-S22N on ER-Golgi cycling of Galtase-YFP and p58-YFP in COS7 cells. (A) Frames from representative photobleach sequences acquired with a confocal microscope as described in Materials and Methods. (B) Frames from similar representative photobleach sequences taken from cells expressing p58-YFP. Cells doubly transfected with p58-YFP and CFP-Rab18-S22N or CFP-Rab18 had a similar appearance. (C) Representative recovery curves showing Golgi-associated Galtase-YFP fluorescence as a function of time in cells singly expressing Galtase-YFP or doubly transfected with Galtase-YFP and CFP-Rab18-S22N. (D) Representative recovery curves show Golgi-associated p58-YFP fluorescence as a function of time in cells singly transfected with p58-YFP or double transfected with p58-YFP and CFP-Rab18 or CFP-Rab18-S22N. Experimental design was as in C. (E) A simple model using pseudo-first-order kinetics to describe cycling of resident Golgi proteins between the ER and Golgi in these experiments. (F) Mean Golgi residence times calculated from photobleach recovery curves and ratios of Golgi/total cellular fluorescence (n>20) transfected with the indicated constructs (Galtase or p58-YFP, CFP-Rab18 or CFP-Rab18-S22N). (G) Mean ER residence times determined from the same cells shown in F. Error bars show s.e.m.

As an alternative measure of retrograde trafficking, we treated COS7 cells transfected with Galtase-YFP and CFP-Rab18-S22N or singly transfected with Galtase-YFP with 5 μg/ml brefeldin A. Brefeldin A induces fusion of Golgi with ER membranes and collapse of the Golgi into the ER in easily observed discrete events termed 'blinkouts' (Sciaky et al., 1997) (Fig. 9A). CFP-Rab18-S22N accelerated the rate of Golgi blinkout relative to single-transfected cells (Fig. 9B,E), consistent with enhancement of fusion of ER with Golgi membranes. In HeLa cells, addition of a pSilencer neo plasmid expressing Rab18-specific siRNA (hsiRNA1) had the reverse effect, inhibiting Golgi-ER fusion in this assay (Fig. 9C,F). CFP-Rab18-S22N-induced enhancement of Golgi/ER fusion still occurred in COS7 cells treated with nocodazole (Fig. 9D), which is more consistent with an increase in fusigenicity (e.g. from enhanced activity of tethers or SNAREs) rather than an increase in motor protein activity (e.g. Rab6/kinesin interactions).

Effects of Rab18 mutants on COPI-dependent retrograde trafficking pathways

Recycling of Galtase-YFP from the Golgi to the ER is not blocked by microinjection of antibodies against COPI, and likely employs a COPI-independent pathway regulated in part by Rab6 (Girod et al., 1999). In contrast, ERGIC53/p58 possesses a dilysine motif which interacts strongly with COPI (Andersson et al., 1999), and requires COPI for retrograde trafficking (Girod et al., 1999).

To monitor effects of overexpression of Rab18 and its mutants on COPI-dependent Golgi-to-ER trafficking of cargo, we examined the COPI-dependent cargo p58-YFP (Presley et al., 2002), the rodent

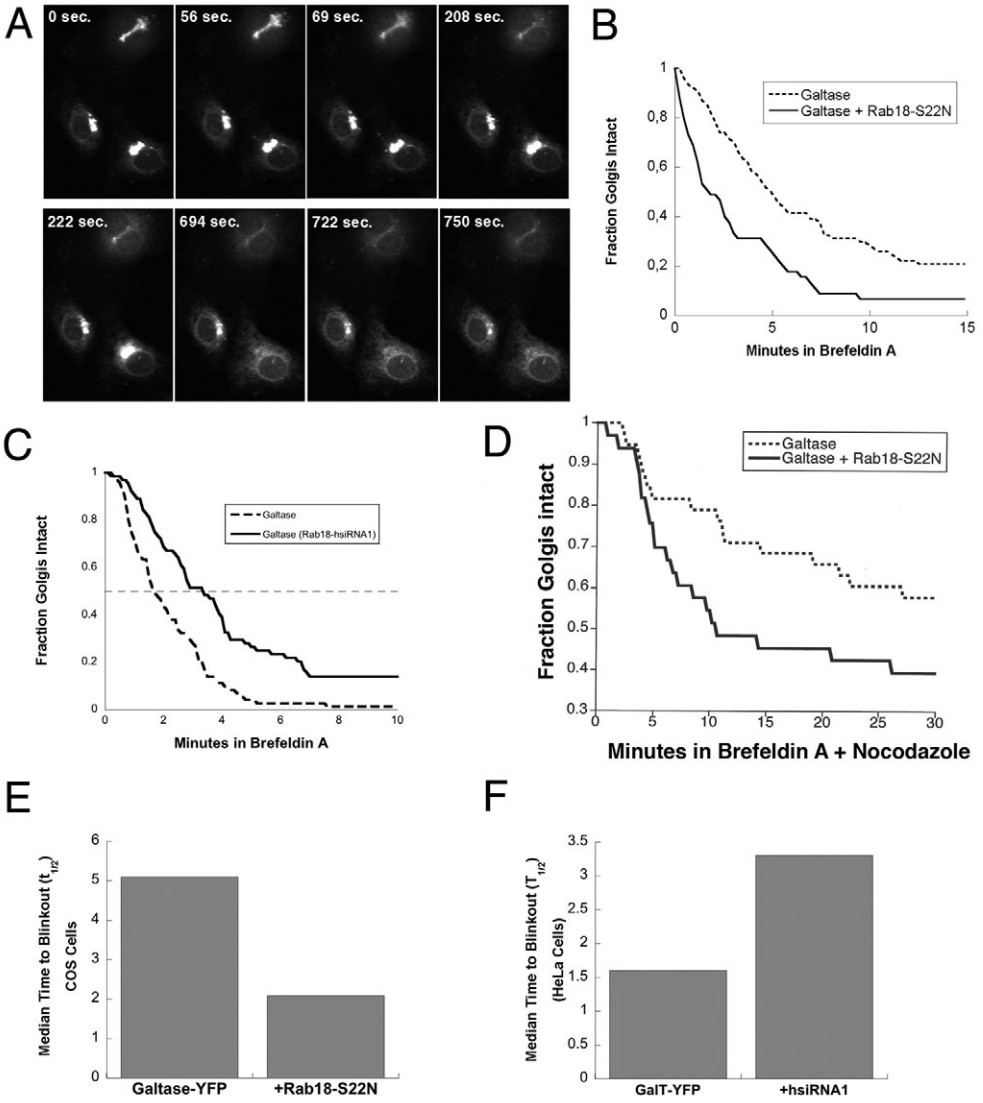

Fig. 9. Effects of Rab18 mutants and knockdowns on rates of brefeldin-A-induced ER-Golgi fusion. (A) Frames taken from a representative time-lapse imaging sequence showing effects of brefeldin A (5 μg/ml)-induced 'blinkout' in COS7 cells expressing Galtase-YFP. (B) Golgis were visualized by Galtase-YFP fluorescence and blinkout after brefeldin A addition and quantified as described (Sciaky et al., 1997). (C) Effects of two siRNAs on rate of Golgi blinkout. hsiRNA1 (expressed from pSilencer Neo) was transiently transfected into HeLa cells. Blinkout was measured as in B, 72 hours after transfection. (D) Quantification of brefeldin-A-induced blinkout in COS7 cells treated with nocodazole and brefeldin A. Cells double-transfected with CFP-Rab18-S22N and Galtase-YFP (48 hours post transfection) were placed on ice for 5 minutes in the presence of nocodozole (1 μg/ml), subsequently they were transferred to a heated microscope stage (37°C) in fresh medium containing both nocodazole and brefeldin A (5 μg/ml). Image sequences were taken as described (Sciaky et al., 1997). (E,F) Quantification of the experiments in B and C, respectively, showing median time to blinkout in cells transfected with the indicated constructs. 100-150 cells were scored for each condition.

analogue of ERGIC53 (Lahtinen et al., 1992). Cells were co-transfected with CFP-Rab18 or CFP-Rab18-S22N or transfected with p58-YFP alone (Fig. 8B) as a control. Anterograde and retrograde cycling between the Golgi and ER were monitored by photobleaching. P58-YFP was found to cycle rapidly between the ER and Golgi consistent with previous findings (Ben-Tekaya et al., 2004; Ward et al., 2001) (Fig. 8D). However, neither anterograde nor retrograde trafficking of p58-YFP was significantly affected by overexpression of CFP-Rab18 or CFP-Rab18-S22N (Fig. 8D,F,G). These data are most compatible with Rab18 function in a COPI-independent pathway from the Golgi complex to the ER.

Discussion

We here utilize new proteomics data obtained from Golgi membranes in order to more systematically study GTPase function with respect to membrane traffic in the early secretory pathway. Of the 32 Arf/Arl/Rab proteins examined in this study, we initially focused on six poorly characterized proteins (Arl6, Rab30, Rab35, Rab43, RabL3 and Rab18). Subsequent more detailed analysis of two proteins, Rab43 and Rab18, now provides strong evidence of involvement in Golgi/ER trafficking pathways.

Role of Rab43 in anterograde trafficking

Further characterization of Rab43 suggested a role in anterograde trafficking of cargo from the ER to the Golgi since a dominant-negative mutant (GFP-Rab43-T32N) produced a striking Golgi redistribution into scattered punctae colocalizing with ER exit sites. Since trafficking of cargo from the ER to the cell surface was not disrupted despite the dramatic Golgi fragmentation, a simple explanation consistent with these data is that Rab43 regulates dynein/dynactin (Burkhardt et al., 1997) or similar proteins required for interaction between pre-Golgi intermediates and microtubules. A similar phenotype is seen when microtubules are disrupted with nocodazole (Cole et al., 1996; Storrie et al., 1998) or when the dynactin complex is disrupted by overexpression of the p50/dynamitin subunit of this complex (Burkhardt et al., 1997). Under these conditions, pre-Golgi intermediates accumulate at ER exit sites where functional Golgi mini-stacks are reconstituted. Some of our experimental results are suggestive of a possible interaction between Rab43 and dynein/dynactin (e.g. Fig. 5D,E).

Others (Haas et al., 2007) have recently published similar experimental results, showing fragmentation of the Golgi without a block in secretion in Rab43-T32N-expressing or Rab43-depleted

cells. They also found a block in the transport of Shiga toxin from the cell surface to the ER when RN-tre, a proposed GAP for Rab43, is overexpressed (Fuchs et al., 2007) and suggested that Rab43 regulates retrograde trafficking from endosomes to Golgi. However, disruption of an endosome/Golgi trafficking pathway would not be expected to dramatically redistribute Golgi elements to COPII-positive ER exit sites (see Fig. 5A). Furthermore, a Rab regulating such a pathway would be expected to show TGN localization, whereas GFP-Rab43 shows an early Golgi localization (see Fig. 2). It is possible that the reduction in Shiga toxin transport could be a secondary consequence of the reorganization of the Golgi complex. Resolving these questions will require further studies including the identification and characterization of Rab43 effectors.

Role of Rab18 in Golgi to ER transport

Rab18 is not found in yeast but has been identified as a Golgi protein in trypanosomes (Jeffries et al., 2002). Rab18 has been localized to endosomes of mammalian cells by antibody staining in previous studies (Lutcke et al., 1994; Yu et al., 1993) and more recently to lipid droplets by multiple techniques including mass spectrometric analysis of purified lipid droplets (Brasaemle et al., 2004; Liu et al., 2004; Umlauf et al., 2004), immunofluorescence (Martin et al., 2005; Ozeki et al., 2005) and immunoelectron microscopy (Martin et al., 2005; Ozeki et al., 2005). Previous to this study, no fundamental generalized role has been proposed for Rab18 in the secretory pathway, although evidence has been provided for a role as a negative regulator of secretion in neuroendocrine cells (Malagon et al., 2005; Vazquez-Martinez et al., 2007).

However, Rab18 was identified by multiple peptides in all rat liver Golgi preparations in two independent proteomic studies (Gilchrist et al., 2006; Wu et al., 2004), consistent with it being an abundant protein on membranes efficiently co-purifying with the Golgi. Liver is a specialized secretory tissue in which ER lipids are transferred to the Golgi at a high rate, necessitating rapid recycling. In cultured cells, we find the predominant localization of Rab18 to be to the ER, consistent with previous studies showing Rab18 to be associated with ER membranes (Gilchrist et al., 2006; Martin et al., 2005). We propose a role in the regulation of membrane recycling back to the ER. Models consistent with such a role can be easily constructed: e.g. if Rab18 recruits a complex (tethers/SNAREs) to ER membranes required for the targeting and fusion of retrograde carriers generated in the Rab6-regulated COPI-independent retrograde pathway.

In this study, overexpression of Rab18 or of Rab18-Q67L resulted in failure of the model cargo protein VSVG to transit the secretory pathway and in severe disruption of the Golgi complex. Similarly, downregulation experiments with a number of independent siRNAs targeting Rab18, also resulted in reduced VSVG transfer to the cell surface and Golgi disorganization. However, the overexpression of Rab18-S22N not only failed to block VSVG transit to the cell surface but rather selectively upregulated the rate of Golgi-to-ER trafficking of Galtase-YFP, which cycles between the Golgi and ER. The overexpression of wild type Rab18 or its GDP/GTP mutants had little effect on Golgi/ER cycling of p58-YFP, which is believed to use a COPI-dependent pathway. Together these results suggest that one function, at least, of Rab18 is in the regulation of COPI-independent recycling to the ER.

We hypothesize that Rab18 acts in the same COPI-independent pathway as Rab6 (Girod et al., 1999), but plays a complementary role, regulating tethering or fusion (most likely on ER membranes) rather than interaction with microtubule motors. Such a role is also consistent with the recent identification of Rab18 on lipid droplets. Indeed, one role proposed for Rab18, to facilitate the association of ER membranes with lipid droplets (Ozeki et al., 2005), could potentially share common mechanisms (e.g. recruitment of tethering proteins by Rab18) with the interaction of Golgi-derived transport intermediates with the ER.

Since Rab18-S22N potentiates BFA-induced Golgi-ER fusion even in cells in which microtubules have been depolymerized, and an siRNA against Rab18 inhibits this fusion, we hypothesize that the function of Rab18 is in the regulation of tethers/SNAREs (analogous to the role of Rab5 in the endocytic pathway). The apparent positive effects of Rab18-S22N may be due to binding of GTP, although at a lower level than wild-type, leading to a less severe phenotype. However, CFP-Rab18-S22N shows membrane association (Fig. 6D) unlike many analogous Rab mutants, which are efficiently extracted from membranes by Rab-GDI while in the GDP form, and it is thus likely that it possesses residual activity. Furthermore, overexpression of a protein required for Golgi-to-ER trafficking could be expected to disrupt the Golgi complex as has been demonstrated for constitutively active Rab6 (Martinez et al., 1997).

Although many years of classical biochemical and genetic studies have provided an excellent understanding of many aspects of secretory pathway function in mammalian cells, this study highlights the importance of embracing new approaches to further our knowledge of the machinery involved. Our identification of roles for Rab18 and Rab43 in ER/Golgi trafficking has been derived from a combination of detailed proteomic analysis of cellular membranes with live-cell imaging and underlines that further work is still necessary to completely elucidate the secretory pathway machinery.

Materials and Methods

Chemicals and supplies

All chemicals were obtained from Sigma-Aldrich (St Louis, MO) unless otherwise stated. Mouse monoclonal anti-actin (1:1000) and mouse monoclonal anti-acetylated tubulin (1:1000) were from Sigma-Aldrich, rabbit polyclonal anti-beta tubulin (1:1000, Abcam, Cambridge, MA), sheep anti-human TGN46 (1:1000; Serotec, Oxford, UK), mouse anti-TGN38 (Affinity Bioreagent, Golden, CO), mouse monoclonal anti-GM130 (1:300; BD Transduction Laboratories, San Diego, CA), rabbit polyclonal anti-mannosidase II (1:300; Chemicon Temecula, CA). Rabbit anti-COPII (Sec23 subunit; 1:300) was a kind gift of Xiaohui Zha (Ridsdale et al., 2006). Rabbit anti-β-COP (1:200) was a kind gift from J. Lippincott-Schwartz (National Institutes of Health, Bethesda, MD). Rabbit anti-p115 (1:100) was a kind gift from E. Sztul (University of Birmingham, AL). Rabbit anti-calnexin (1:50) was a kind gift from Ali Fazel (Montreal, CA), The anti-VSVG antibody VG was obtained from hybridoma cells previously described (Liebel et al., 2003). Secondary antibodies included goat-anti-rabbit/mouse conjugated to Cy3/Cy5 (Chemicon, Temecula, CA) and donkey anti-sheep IgG antibodies (Alexa Fluor 568; Molecular Probes, Invitrogen, Burlington, ON). Secondary antibodies were used at 1:300 for immunofluorescence, unless specified. Cy3-conjugated chrompure human transferrin (25 μg/ml) was purchased from Jackson ImmunoResearch, Mississauga, ON. Texas Red EGF (100 ng/ml), DAPI and TO-PRO-3 iodide (1:1000) and phalloidin (1:10,000) were obtained from Molecular Probes.

Plasmid construction

Human cDNA clones containing the open reading frames of GTPases not already GFP tagged were obtained from the RZPD (Berlin, Germany) and GFP tagged as summarized in supplementary material Table S1.

Human specific hairpin siRNA template oligonucleotide, hsiRNA1 (AATCGTGAAGGTCGATAGAAAT) was expressed in the pSilencer Neo^{TM} plasmid (Ambion, Austin, TX). siRNA oligonucleotides siRab18-1 and siRab18-2 were from Ambion (siRNA 120633; 120635). siRab18-3 was from Qiagen (siRNA si02662709). Oligonucleotides were transfected using Oligofectamine (Invitrogen) according to the manufacturer's instructions.

Cell culture and transfection

COS7, HeLa, Normal Rat Kidney (NRK) and Vero cells were grown in Dulbecco's Modified Eagle Medium (DMEM) supplemented with 10% fetal calf serum, 2 mM glutamine, 150 mg/ml penicillin and 100 U/ml streptomycin (Invitrogen, Burlington, ON). Cells were kept in an incubator at 37°C with 5% CO_2.

Cells were grown to 40-80% confluence on glass coverslips in six-well plates and transfected using FuGENE 6 reagent (Roche Diagnostics, Indianapolis, IN) or Lipofectamine 2000 (Invitrogen) according to the manufacturer's instructions. All plasmids were purified using Qiagen plasmid purification kits (Qiagen, Mississauga, ON).

Immunofluorescence, live-cell imaging and microscopy

Cells were incubated for 24 hours after transfection at 37°C to allow expression of the GFP construct, fixed in 4% paraformaldehyde in PBS (pH 7.2) (PFA/PBS) for 10 minutes, and washed with PBS containing 25 mM glycine (10 minutes), with two subsequent washes with PBS (10 minutes each). Cells were then permeabilized with 0.1% Triton X-100 for 5 minutes then washed three times in PBS and placed in medium containing 3% heat-inactivated normal goat serum (NGS; Invitrogen, Burlington, ON) PBS (NGS/PBS) for 60 minutes. Cells were incubated with primary antibody diluted in NGS/PBS for 1 hour followed by three washes in PBS and subsequent incubation with secondary antibody. Cells were washed three times with PBS, and finally mounted on slides with Geltol mounting medium (Immunon, Shandon, Pittsburgh, PA) for immunofluorescence.

For live imaging, cells were plated onto coverslip bottom dishes (MatTek Inc, Ashland, MA) or LabTek chambers (Nalge Nunc, Rochester, NY). MatTek dishes were maintained during imaging at 37°C using a Zeiss CO_2-controlled live-cell chamber. LabTek chambers were maintained at 37°C on the microscope stage using a Nevtek air stream incubator (Nevtek, Williamsville, VA).

Unless otherwise stated, images were taken using a Zeiss LSM510 confocal microscope using a NA 1.4 63× oil-immersion objective lens with the pinhole set at 0.7-1.0 Airy units and slice thickness matched in all channels. GFP and Alexa Fluor 488 were visualized using 488 nm excitation and a BP 505-530 nm emission filter. Cy3 was visualized using 543 nm excitation and a BP 560-615 nm emission filter. Cy5 was visualized using 633 nm excitation and a 650 nm long-pass for emission. CFP fluorescence was excited using 405 nm excitation and a 470-500 nm band-pass emission filter. A 25× Neofluar variable immersion lens (NA 0.8) with fully open pinhole was used for quantitative live cell imaging experiments where all fluorescence in the cell must be accounted for (i.e. all experiments involving photobleach).

Golgi fragmentation was quantified based on published methods (Liebel et al., 2003) and fragmentation normalized to nontransfected cells (1 by definition). To compute Golgi dispersal for a single cell, the average position of the GM130 fragments weighed by fragment intensity ('Golgi centroid') was computed. A radius (r) from the Golgi centroid encompassing sufficient GM130 fragments to account for 50% of the total Golgi intensity was calculated. The area was then calculated (πr^2). This area was normalized to Golgi complex in nontransfected cells in the same experiment (1 by definition) to give a relative measure of Golgi dispersal. Absolute cellular fluorescence was calculated in equivalent molecules of fluorescein using published methods (Piston et al., 1999).

Quantification of VSVG trafficking to the cell surface

COS7 cells grown on coverslips were singly transfected with VSVG-YFP/CFP or doubly transfected with VSVG-YFP/CFP and a GFP/CFP-tagged Rab construct and incubated for 24 or 48 hours at 40°C to accumulate VSVG-YFP/CFP in the ER. Cells were then shifted to 32°C for varying times (0, 1 or 3 hours) allowing VSVG to traffic to the cell surface. Samples were subsequently fixed and processed for immunofluorescence as described above using a mouse monoclonal antibody directed against an epitope on the luminal portion of the VSVG-YFP/CFP molecule (VG antibody). Alternatively, cells were stained with the VG antibody (Liebel et al., 2003) as above but without permeabilization. Labeling was subsequently visualized in either case using a Cy3-labeled secondary antibody. Without permeabilization, VG fails to stain intracellular VSVG (Liebel et al., 2003). Total VSVG staining including the ER and Golgi pools can be visualized either by fluorescence of the YFP/CFP tag or by permeabilization prior to staining with VG. 12-bit confocal images were acquired from all samples within a single experiment using identical settings and a 25× NA 0.7 oil-immersion objective with fully open pinhole.

The boundaries of transfected cells were outlined using Metamorph, background corrected using a region of interest outside any cell, and the ratio of VG/YFP fluorescence calculated. This ratio was normalized to 1.0 for control cells transfected with VSVG-YFP alone.

Measurement of rates of trafficking of Galtase-YFP and p58-YFP between ER and Golgi

COS7 cells in MatTek chambers were transfected with Galtase-YFP or p58-YFP alone or in combination with a Rab18 CFP construct (CFP-Rab18 or dominant-negative CFP-Rab18-S22N), incubated for 48 hours and subsequently transferred to a live imaging chamber (Carl Zeiss GmbH, Jena Germany) with 5% CO_2 and held at 37°C on the stage of a LSM Zeiss 510 confocal microscope. Photobleach sequences (45 minutes total length) were acquired and recovery curves obtained as described (Presley, 2005) using a 25× NA 0.7 objective with fully open pinhole. The methods described in detail (Presley, 2005) were used to obtain forward and reverse rate constants between the ER and Golgi.

We wish to thank David Stephens for plasmid expressing GFP-p150^{Glued}, Elizabeth Sztul for antibodies directed against p115, Jennifer Lippincott-Schwartz for antibodies directed against COPI, Xiaohui Zha for antibodies directed against COPII, and Ali Fazel for antibodies directed against calnexin. We thank Marieve Picard for her help. We also wish to thank Richard Vo, Charlie Koop and Brigitte Joggerst for technical assistance. We wish to thank Eric Danek, Ryan Petrie, and Arturo Mancini for helpful discussion and critical reading of the manuscript and members of the Bergeron laboratory for pre-publication access to data from MASCOT analysis. Members of the Lamarche-Vane lab provided support and encouragement for which we are grateful. This research was supported by grants from the Canadian Institutes for Health Research (MOP-49590 and PRG-80153) and the National Institutes of Health (R21-GM070588).

References

Andersson, H., Kappeler, F. and Hauri, H. P. (1999). Protein targeting to endoplasmic reticulum by dilysine signals involves direct retention in addition to retrieval. *J. Biol. Chem.* **274**, 15080-15084.

Babbey, C. M., Ahktar, N., Wang, E., Chen, C. C., Grant, B. D. and Dunn, K. W. (2006). Rab10 regulates membrane transport through early endosomes of polarized Madin-Darby canine kidney cells. *Mol. Biol. Cell* **17**, 3156-3175.

Behnia, R., Panic, B., Whyte, J. R. C. and Munro, S. (2004). Targeting of the Arf-like GTPase Arl3p to the Golgi requires N-terminal acetylation and the membrane protein Sys1p. *Nat. Cell Biol.* **6**, 405-413.

Ben-Tekaya, H., Miura, K., Pepperkok, R. and Hauri, H. P. (2004). Live imaging of bidirectional traffic from the ERGIC. *J. Cell Sci.* **118**, 357-367.

Blobel, G. and Dobberstein, B. (1975). Transfer of proteins across membranes. I. Presence of proteolytically processed and unprocessed nascent immunoglobulin light chains on membrane-bound ribosomes of murine myeloma. *J. Cell Biol.* **67**, 835-851.

Brasaemle, D. L., Dolios, G., Shapiro, L. and Wang, R. (2004). Proteomic analysis of proteins associated with lipid droplets of basal and lipolytically stimulated 3T3-L1 adipocytes. *J. Biol. Chem.* **279**, 46835-46842.

Burkhardt, J. K., Echeverri, C. J., Nilsson, T. and Vallee, R. B. (1997). Overexpression of the dynamitin (p50) subunit of the dynactin complex disrupts dynein-dependent maintenance of membrane organelle distribution. *J. Cell Biol.* **139**, 469-484.

Chavrier, P., Parton, R. G., Hauri, H. P., Simons, K. and Zerial, M. (1990). Localization of low molecular weight GTP binding proteins to exocytic and endocytic compartments. *Cell* **62**, 317-329.

Chen, Y.-T., Holcomb, C. and Moore, H. P. H. (1993). Expression and localization of two low molecular weight GTP-binding proteins, Rab8 and Rab10 by epitope tag. *Proc. Natl. Acad. Sci. USA* **90**, 6508-6512.

Christoforidis, S., McBride, H. M., Burgoyne, R. D. and Zerial, M. (1999). The Rab5 effector EEA1 is a core component of endosome docking. *Nature* **397**, 621-625.

Cole, N. B., Sciaky, N., Marotta, A., Song, J. and Lippincott-Schwartz, J. (1996). Golgi dispersal during microtubule disruption: regeneration of Golgi stacks at peripheral endoplasmic reticulum exit sites. *Mol. Biol. Cell* **7**, 631-650.

de Leeuw, H. P., Koster, P. M., Calafat, J., Janssen, H., van Zonneveld, A. J., van Mourik, J. A. and Voorberg, J. (1998). Small GTP-binding proteins in human epithelial cells. *Brit. J. Haematol.* **103**, 15-19.

De Renzis, S., Sonnichsen, B. and Zerial, M. (2002). Divalent Rab effectors regulate the sub-compartmental organization and sorting of early endosomes. *Nat. Cell Biol.* **4**, 124-133.

Dejgaard, S. Y., Murshid, A., Dee, K. M. and Presley, J. F. (2007). Confocal microscopy based linescan methodologies for intra-Golgi localization of proteins. *J. Histochem. Cytochem.* **55**, 709-719.

Deretic, D., Williams, A. H., Ransom, N., Morel, V., Hargrave, P. A. and Arendt, A. (2005). Rhodopsin C terminus, the site of mutations causing retinal disease, regulates trafficking by binding to ADP-ribosylation factor 4 (ARF4). *Proc. Natl. Acad. Sci. USA* **102**, 3301-3306.

Donaldson, J. G., Honda, A. and Weigert, R. (2005). Multiple activities for Arf1 at the Golgi complex. *Biochim. Biophys. Acta* **1744**, 364-373.

Echard, A., Jollivet, F., Martinez, O., Lacapere, J. J., Rousselet, A., Janoueix-Lerosey, I. and Goud, B. (1998). Interaction of a Golgi-associated kinesin-like protein with Rab6. *Science* **279**, 580-585.

Fuchs, E., Haas, A. K., Spooner, R. K., Yoshimura, S., Lord, J. M. and Barr, F. A. (2007). Specific Rab GTPase-activating proteins define the Shiga toxin and epidermal growth factor uptake pathways. *J. Cell Biol.* **177**, 1133-1143.

Gilchrist, A., Au, C. E., Hiding, J., Bell, A. W., Fernandez-Rodriguez, J., Lesimple, S., Nagaya, H., Roy, L., Calafel, S. J., Hallet, M. et al. (2006). Quantitative proteomic analysis of the secretory pathway. *Cell* **127**, 1265-1281.

Girod, A., Storrie, B., Simpson, J. C., Johannes, L., Goud, B., Roberts, L. M., Lord, J. M., Nilsson, T. and Pepperkok, R. (1999). Evidence for a COP-I-independent

transport route from the Golgi complex to the endoplasmic reticulum. *Nature Cell Biol.* **1**, 423-430.
Golgi, C. (1898). Sur la structure des cellules nerveuses. *Arch. Ital. Biol.* **30**, 60-71.
Goud, B., Zahraoui, A., Tavitian , A. and Saraste, J. (1990). Small GTP-binding protein associated with Golgi cisternae. *Nature* **345**, 553-556.
Haas, A. K., Fuchs, E., Kopajtich, R. and Barr, F. A. (2005). A GTPase-activating protein controls Rab5 function in endocytic trafficking. *Nat. Cell Biol.* **7**, 887-893.
Haas, A. K., Yoshimura, S., Stephens, D. J., Presisinger, C., Fuchs, E. and Barr, F. A. (2007). Analysis of GTPase-activating proteins: Rab1 and Rab43 are key Rabs required to maintain a functional Golgi complex in human cells. *J. Cell Sci.* **120**, 2997-3010.
Hosaka, M., Tosa, K., Takatsu, H., Toril, S., Murakami, K. and Nakayama, K. (1996). Structure and intracellular localization of mouse ADP-ribosylation factors type 1 to type 6 (ARF1-ARF6). *J. Biochem.* **120**, 813-819.
Huang, C. F., Buu, L., Yu, W. and Lee, F. (1999). Characterization of a novel ADP-ribosylation factor like protein (yARL3) in Saccharomyces cerevisiae. *J. Biol. Chem.* **274**, 3819-3827.
Huber, L. A., Pimplikar, S., Parton, R. G., Virta, H., Zerial, M. and Simons, K. (1993). Rab8, a small GTPase involved in vesicular traffic between the TGN and the basolateral plasma membrane. *J. Cell Biol.* **123**, 35-45.
Ingley, E., Williams, J. H., Walker, C. E., Tsai, S., Colley, S., Sayer, M. S., Tilbrook, P. A., Sarna, M., Beaumont, J. C. and Klinken, S. P. (1999). A novel ADP-ribosylation like factor (ARL-6) interacts with the protein-conducting channel SEC61beta subunit. *FEBS Lett.* **459**, 69-74.
Jeffries, T. R., Morgan, G. W. and Field, M. C. (2002). TbRAB18, a developmentally regulated Golgi GTPase from Trypanosoma brucei. *Mol. Biochem. Parasitol.* **121**, 63-74.
Jiang, S. and Storrie, B. (2005). Cisternal Rab proteins regulate Golgi apparatus redistribution in response to hypotonic stress. *Mol. Biol. Cell* **16**, 2586-2596.
Junutula, J. R., De Maziére, A. M., Peden, A. A., Ervin, K. E., Advani, R. J., van Dijk, S. M., Klumperman, J. and Scheller, R. H. (2004). Rab14 is involved in membrane trafficking between the Golgi complex and endosomes. *Mol. Biol. Cell* **15**, 2218-2229.
Kahn, R. A., Cherfils, J., Elias, M., Lovering, R. C., Munro, S. and Schurmann, A. (2006). Nomenclature for the human Arf family of GTP-binding proteins: ARF, ARL and SAR proteins. *J. Cell Biol.* **172**, 645-650.
Kouranti, I., Sachse, M., Arouche, N., Goud, B. and Echard, A. (2006). Rab35 regulates an endocytic recycling pathway essential for the terminal steps of cytokinesis. *Curr. Biol.* **16**, 1719-1725.
Lahtinen, U., Dahllof, B. and Saraste, J. (1992). Characterization of a 58 kDa cis-Golgi protein in pancreatic exocrine cells. *J. Cell Sci.* **111**, 321-333.
Lazar, T., Gotte, M. and Gallwitz, D. (1997). Vesicular transport: how many Ypt/Rab-GTPases make a eukaryotic cell. *Trends Biochem. Sci.* **22**, 468-472.
Liebel, U., Starkuviene, V., Erfle, H., Simpson, J. C., Poustka, A., Wiemann, S. and Pepperkok, R. (2003). A microscope-based screening platform for large-scale functional protein analysis in intact cells. *FEBS Lett.* **554**, 394-398.
Liu, P., Ying, Y., Zhao, Y., Mundy, D. I., Zhu, M. and Anderson, R. G. W. (2004). Chinese hamster ovary K2 cell lipid droplets appear to be metabolic organelles involved in membrane traffic. *J. Biol. Chem.* **279**, 3787-3792.
Lombardi, D., Soldati, R., Riederer, M. A., Goda, Y., Zerial, M. and Pfeffer, S. R. (1993). Rab9 functions in transport between late endosomes and the trans Golgi network. *EMBO J.* **12**, 677-682.
Lowe, S. L., Wong, S. H. and Hong, W. (1996). The mammalian ARF-like protein 1 (Arl1) is associated with the Golgi complex. *J. Cell Sci.* **109**, 209-220.
Lutcke, A., Parton, R. G., Murphy, C., Olkkonen, V. M., Dupree, P., Valencia, A., Simons, K. and Zerial, M. (1994). Cloning and subcellular localization of novel rab proteins reveals polarized and cell type-specific expression. *J. Cell Sci.* **107**, 3437-3448.
Malagon, M. M., Cruz, D., Vazquez-Martinez, R., Pienado, J. R., Anouar, Y., Tonon, M. C., Vaudry, H., Gracia-Navarro, F. and Castano, J. P. (2005). Analysis of Rab18 and a new Golgin in the secretory pathway. *Ann. N. Y. Acad. Sci.* **1040**, 137-139.
Mallard, F., Tang, B. L., Galli, T., Saint-Pol, A., Yue, X., Antony, C., Hong, W., Goud, B. and Johannes, L. (2002). Early/recycling endosomes-to-TGN transport involves two SNARE complexes and a Rab6 isoform. *J. Cell Biol.* **156**, 653-664.
Martin, S., Driessen, K., Nixon, S. J., Zerial, M. and Parton, R. G. (2005). Regulated localization of Rab18 to lipid droplets. *J. Biol. Chem.* **280**, 42325-42335.
Martinez, O., Antony, C., Perhau-Arnaudet, G., Berger, E. G., Salamero, J. and Goud, B. (1997). GTP-bound forms of rab6 induce the redistribution of Golgi proteins into the endoplasmic reticulum. *Proc. Natl. Acad. Sci. USA* **94**, 1828-1833.
McBride, H. M., Rybin, V., Murphy, C., Giner, A., Teasdale, R. and Zerial, M. (1999). Oligomeric complexes link Rab5 effectors with NSF and drive membrane fusion via interactions between EEA1 and syntaxin 13. *Cell* **98**, 377-386.
Mellman, I. and Simons, K. (1992). The Golgi complex: in vitro veritas? *Cell* **68**, 829-840.
Michaelson, D., Silletti, J., Murphy, G., D'Eustachio, P., Rush, M. and Philips, M. R. (2001). Differential localization of Rho GTPases in live cells: regulation by hypervariable regions and RhoGDI binding. *J. Cell Biol.* **152**, 111-126.
Ohta, Y., Suzuki, N., Nakamura, S., Hartwig, J. H. and Stossel, T. P. (1999). The small GTPase RalA targets filamin to induce filopodia. *Proc. Natl. Acad. Sci. USA* **96**, 2122-2128.
Olkkonen, V. M., Dupree, P., Killisch, I., Lütcke, A., Zerial, M. and Simons, K. (1993). Molecular cloning and subcellular localization of three GTP-binding proteins of the rab subfamily. *J. Cell Sci.* **106**, 1249-1261.
Opdam, F. J. M., Echard, A., Croes, H. J., van den Hurk, J. A., van de Vorstenbosch, R. A., Ginsel, L. A., Goud, B. and Fransen, J. A. (2000). The small GTPase Rab6B, a novel Rab6 subfamily member, is cell-type specifically expressed and localised to the Golgi apparatus. *J. Cell Sci.* **113**, 2725-2735.
Orci, L., Perrelet, A., Ravazzola, M., Wieland, F. T., Schekman, R. and Rothman, J. E. (1993). "BFA bodies": a subcompartment of the endoplasmic reticulum. *Proc. Natl. Acad. Sci. USA* **90**, 11089-11093.
Ozeki, S., Cheng, J., Tauchi-Sato, K., Hatano, N., Taniguchi, H. and Fujimoto, T. (2005). Rab18 localizes to lipid droplets and induces their close apposition to the endoplasmic reticulum-derived membrane. *J. Cell Sci.* **118**, 2601-2611.
Palade, G. E. (1975). Intracellular aspects of the process of protein synthesis. *Science* **189**, 347-356.
Pereira-Leal, J. B. and Seabra, M. C. (2001). Evolution of the Rab family of small GTP-binding proteins. *J. Mol. Biol.* **313**, 889-901.
Piston, D. W., Patterson, G. H. and Knobel, S. M. (1999). Quantitative imaging of the green fluorescent protein (GFP). *Methods Cell Biol.* **58**, 31-48.
Pizon, V., Desjardins, M., Bucci, C., Parton, R. G. and Zerial, M. (1994). Association of Rap1a and Rap1b proteins with late endocytic/phagocytic compartments and Rab2a with the Golgi complex. *J. Cell Sci.* **107**, 1661-1670.
Plutner, H., Cox, A. D., Pind, S., Khosravi-Far, R., Bourne, J. R., Schwaninger, R., Der, C. J. and Balch, W. E. (1991). Rab1b regulates vesicular transport between the endoplasmic reticulum and successive Golgi compartments. *J. Cell Biol.* **115**, 31-43.
Porter, K. R., Claude, A. and Fullam, E. (1945). A study of tissue culture cells by electron microscopy. Methods and preliminary observations. *J. Exp. Med.* **81**, 233-241.
Presley, J. F. (2005). Measurement of protein motion by photobleaching. In: *Cell Imaging: Methods Express Series* (ed. D. Stephens), pp. 119-144. Oxford: Scion Publishing.
Presley, J. F., Cole, N. B., Schroer, T. A., Hirschberg, K., Zaal, K. J. M. and Lippincott-Schwartz, J. (1997). ER-to-Golgi trafficking visualized in living cells. *Nature* **389**, 81-85.
Presley, J. F., Ward, T. H., Pfeifer, A. C., Siggia, E. D., Phair, R. D. and Lippincott-Schwartz, J. (2002). Dissection of COPI and Arf1 dynamics *in vivo* and role in Golgi membrane transport. *Nature* **417**, 187-193.
Ridsdale, A., Denis, M., Gougeon, P.-Y., Ngsee, J. K., Presley, J. F. and Zha, X. (2006). Cholesterol is required for efficient endoplasmic reticulum-to-Golgi transport of secretory membrane proteins. *Mol. Biol. Cell* **17**, 1593-1605.
Sciaky, N., Presley, J. F., Smith, C. L., Zaal, K. J. M., Cole, N. B., Moreira, J. E., Terasaki, M., Siggia, E. and Lippincott-Schwartz, J. (1997). Golgi tubule traffic and the effects of brefeldin A visualized in living cells. *J. Cell Biol.* **139**, 1137-1155.
Sciorra, V. A., Audhya, A., Parsons, A. B., Segev, N., Boone, C. and Emr, S. D. (2005). Synthetic genetic array analysis of the PtdIns 4-kinase Pik1p identifies components in a Golgi-specific Ypt31/rab-GTPase signaling pathway. *Mol. Biol. Cell* **16**, 776-793.
Shin, H.-W., Kobayashi, H., Kitamura, M., Waguri, S., Suganuma, T., Uchiyama, Y. and Nakayama, K. (2005). Roles of ARFRP1 (ADP-ribosylation factor-related protein 1) in post-Golgi membrane trafficking. *J. Cell Sci.* **118**, 4039-4048.
Simpson, J. C., Griffiths, G., Wessling-Resnick, M., Fransen, J. A., Bennett, H. and Jones, A. T. (2004). A role for the small GTPase Rab21 in the early endocytic pathway. *J. Cell Sci.* **117**, 6297-6311.
Simpson, J. C., Cetin, C., Erfle, H., Joggerst, B., Liebel, U., Ellenberg, J. and Pepperkok, R. (2007). An RNAi screening platform to identify secretion machinery in mammalian cells. *J. Biotechnol.* **129**, 352-365.
Sonnichsen, B., De Renzis, S., Nielsen, E., Rietdorf, J. and Zerial, M. (2000). Distinct membrane domains on endosomes in the recycling pathway visualized by multicolor imaging of Rab4, Rab5 and Rab11. *J. Cell Biol.* **149**, 901-914.
Stearns, T., Willingham, M. C., Botstein, D. and Kahn, R. A. (1990). ADP-ribosylation factor is functionally and physically associated with the Golgi complex. *Proc. Natl. Acad. Sci. USA* **87**, 1238-1242.
Stenmark, H. and Olkkonen, V. M. (2001). The Rab GTPase family. *Genome Biol.* **2**, 1-7.
Storrie, B., White, J., Roettger, J. S., Stelzer, E. H. K., Suganuma, T. and Nilsson, T. (1998). Recycling of Golgi resident glycosyltransferases through the ER reveals a novel pathway and provides an explanation for nocodazole-induced Golgi scattering. *J. Cell Biol.* **143**, 1505-1521.
Sztul, E. and Lupashin, V. (2006). Role of tethering factors in secretory membrane traffic. *Am. J. Physiol. Cell Physiol.* 290, C11-C26.
Teal, S. B., Hsu, V. W., Peters, P. J., Klausner, R. D. and Donaldson, J. G. (1994). An activating mutation in ARF1 stabilizes coatomer binding to Golgi membranes. *J. Biol. Chem.* **269**, 3135-3138.
Tian, K., Jurukovski, V., Yuan, L., Shan, J. and Xu, H. (2005). WTH3, which encodes a small G protein, is differentially regulated in multidrug-resistant and sensitive MCF7 cells. *Cancer Res.* **65**, 7421-7428.
Tsai, S.-C., Adamik, R., Haun, R. S., Moss, J. and Vaughan, M. (1992). Differential interaction of ADP-ribosylation factors 1, 3 and 5 with rat brain Golgi membranes. *Proc. Natl. Acad. Sci. USA* **89**, 9272-9276.
Ullrich, O., Reinsch, S., Urbe, S., Zerial, M. and Parton, R. G. (1996). Rab11 regulates recycling through the pericentriolar recycling endosome. *J. Cell Biol.* **135**, 913-924.
Umlauf, E., Csaszar, E., Moertelmaier, M., Schuetz, G. J., Parton, R. G. and Prohaska, R. (2004). Association of stomatin with lipid bodies. *J. Biol. Chem.* **279**, 23699-23709.
Valsdottir, R., Hashimoto, H., Ashman, K., Koda, T., Storrie, B. and Nilsson, T. (2001). Identification of rabaptin-5, rabex-5, and GM130 as putative effectors of rab33b, a regulator of retrograde traffic between the Golgi apparatus and ER. *FEBS Lett.* **508**, 201-209.
Van Der Sluijs, P., Hull, M., Zahraoui, A., Tavitian, A., Goud, B. and Mellman, I. (1991). The small GTP-binding protein rab4 is associated with early endosomes. *Proc. Natl. Acad. Sci. USA* **88**, 6313-6317.
Vazquez-Martinez, R., Cruz-Garcia, D., Duran-Prado, M., Peinado, J. R., Castano, J. P. and Malagon, M. M. (2007). Rab18 inhibits secretory activity in neuroendocrine cells by interacting with secretory granules. *Traffic* **8**, 867-882.

Vieira, O. V., Bucci, C., Harrison, R. E., Trimble, W. S., Lanzetti, L., Gruenberg, J., Schreiber, A. D., Stahl, P. D. and Grinstein, S. (2003). Modulation of Rab5 and Rab7 recruitment to phagosomes by phosphadylinositol 3-kinase. *Mol. Cell. Biol.* **23**, 2501-2514.

Ward, T. H., Polishchuk, R. S., Caplan, S., Hirschberg, K. and Lippincott-Schwartz, J. (2001). Maintenance of Golgi structure and function depends on the integrity of ER export. *J. Cell Biol.* **155**, 557-570.

Watson, P. and Stephens, D. J. (2006). Microtubule plus-end loading of p150(Glued) is mediated by EB1 and CLIP-170 but is not required for intracellular membrane traffic in mammalian cells. *J. Cell Sci.* **119**, 2758-2767.

White, J., Johannes, L., Mallard, F., Girod, A., Grill, S., Reinsch, S., Keller, P., Tzschaschel, B., Echard, A., Goud, B. et al. (1999). Rab6 coordinates a novel Golgi to ER retrograde transport pathway in live cells. *J. Cell Biol.* **147**, 743-759.

Wu, C. C., MacCoss, M. J., Mardones, G., Finnigan, C., Mogelsvang, S., Yates, J. R. and Howell, K. E. (2004). Organellar proteomics reveals Golgi arginine dimethylation. *Mol. Biol. Cell* **15**, 2907-2919.

Yu, H., Leaf, D. S. and Moore, H. P. H. (1993). Gene cloning and characterization of a GTP-binding Rab protein from mouse pituitary AtT-20 cells. *Gene* **132**, 273-278.

Zaal, K. J. M., Smith, C. L., Polishchuk, R. S., Altan, N., Cole, N. B., Ellenberg, J., Hirschberg, K., Presley, J. F., Roberts, T. H., Siggia, E. et al. (1999). Golgi membranes are absorbed into and reemerge from the ER during mitosis. *Cell* **99**, 589-601.

Zahn, C., Hommel, A., Lu, L., Hong, W., Walther, D. J., Florian, S., Joost, H. G. and Schürmann, A. (2006). Knockout of Arfrp1 leads to disruption of ARF-like1 (ARL1) targeting to the trans-Golgi in mouse embryos and HeLa cells. *Mol. Membr. Biol.* **23**, 475-485 .

Zerial, M. and McBride, H. (2001). Rab proteins as membrane organizers. *Nature Rev. Mol. Cell. Biol.* **2**, 107-117.

Zheng, J. Y. Koda, T., Fujiwara, T., Kishi, M., Ikehara, Y. and Kakinuma, M. (1998). A novel Rab GTPase, Rab33B, is ubiquitously expressed and localized to the medial Golgi cisternae. *J. Cell Sci.* **111**, 1061-1069.

Zuk, P. A. and Elferink, L. A. (1999). Rab15 mediates an early endocytic event in Chinese hamster ovary cells. *J. Biol. Chem.* **274**, 22303-22312..

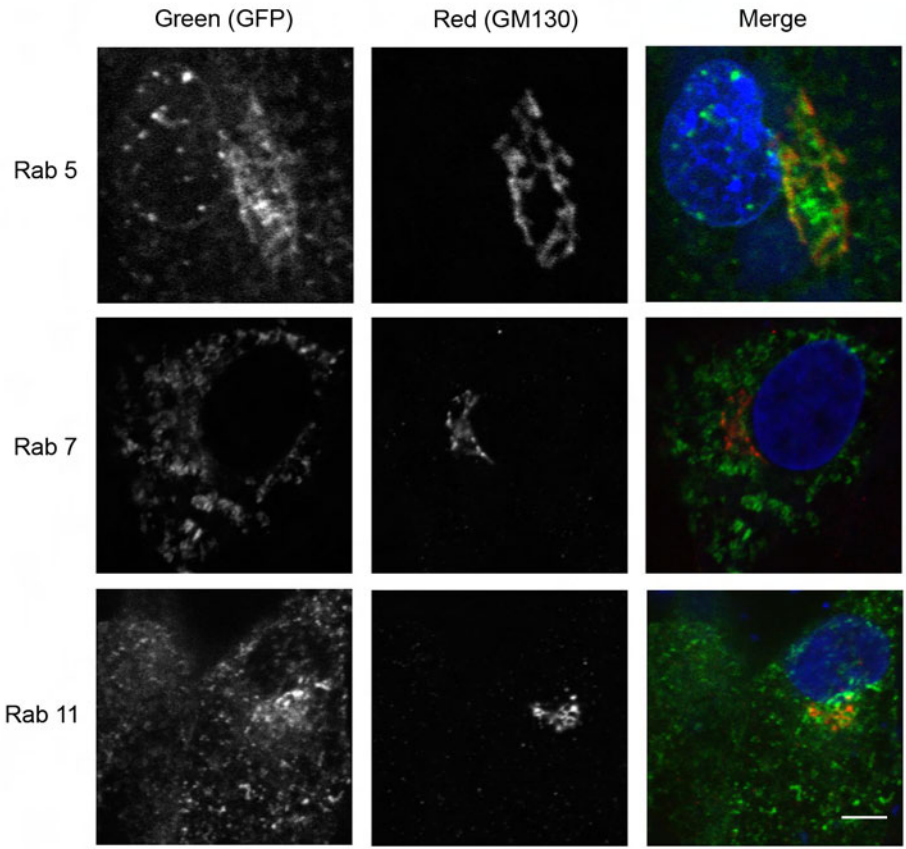

Supplemental Figure 1. Comparison of distributions of endosomal Rabs with Golgi markers. Vero cells were transfected with the indicated GFP constructs. Nuclei and GM130 were visualized as described in Fig. 1 in the main text. Scale bar represents 5 μm.

A. Fully automated intra-Golgi localization (nocodazole ministacks).

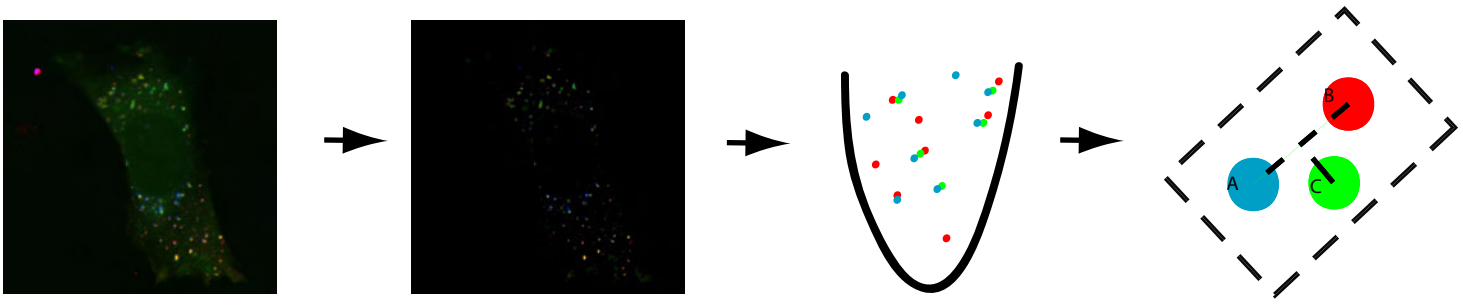

B. Results for Rabs/Arls (NRK cells)

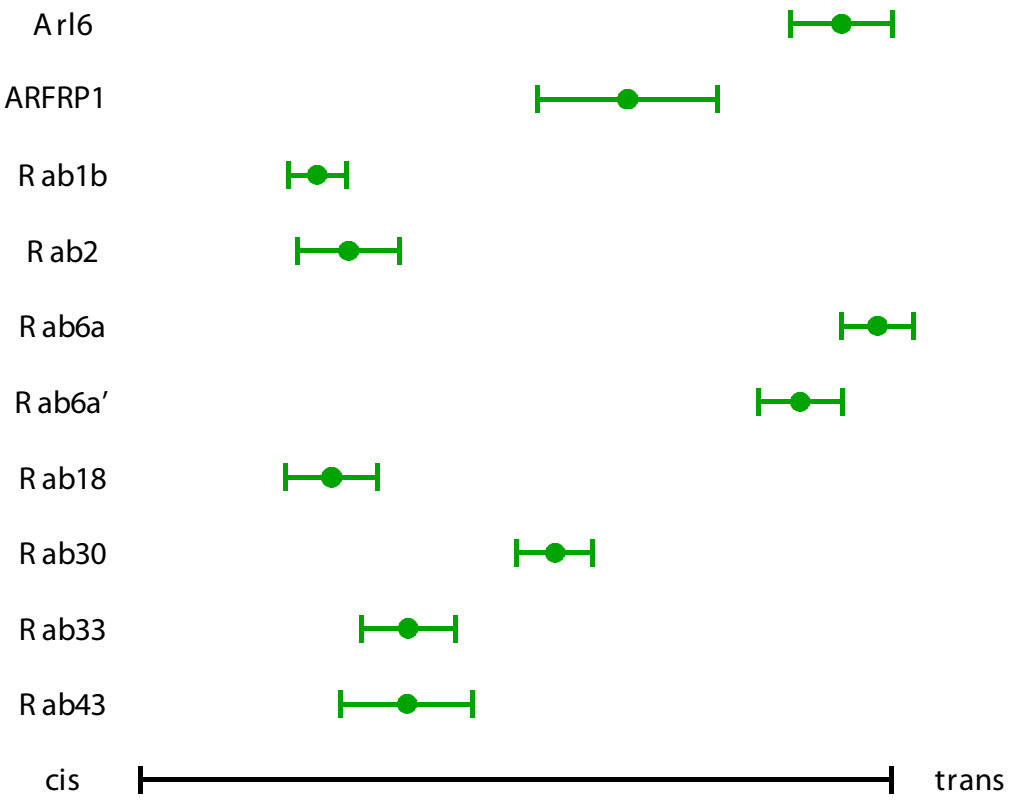

Supplemental Figure 2. Light Microscopic Localization of Rab Proteins to Golgi Subdomains in Nocodazole-Treated NRK Cells. NRK cells transfected with the indicated GFP-Rab constructs were incubated 5 hrs. in 1 µg/ml nocodazole starting at 19 hrs post-transfection to disperse the Golgi into mini-stacks. Cells were fixed and stained for p115 and TGN38 and imaged as described in the main text. Location of the GFP-Rab within each mini-stack was scored using a fully automated procedure as described in detail elsewhere (Dejgaard et al., 2007), and values for each mini-stack scored averaged to produce a value for each cell. This procedure is briefly illustrated in (A). (B) Results of analysis. 15 – 25 cells were scored for each protein. Values were then rescaled to match the average value of the cis control (an average of Rab1b and Rab2) and the trans control (average of Rab6a and Rab6a') to the values in Fig. 3. Error bars indicate s.e.m.

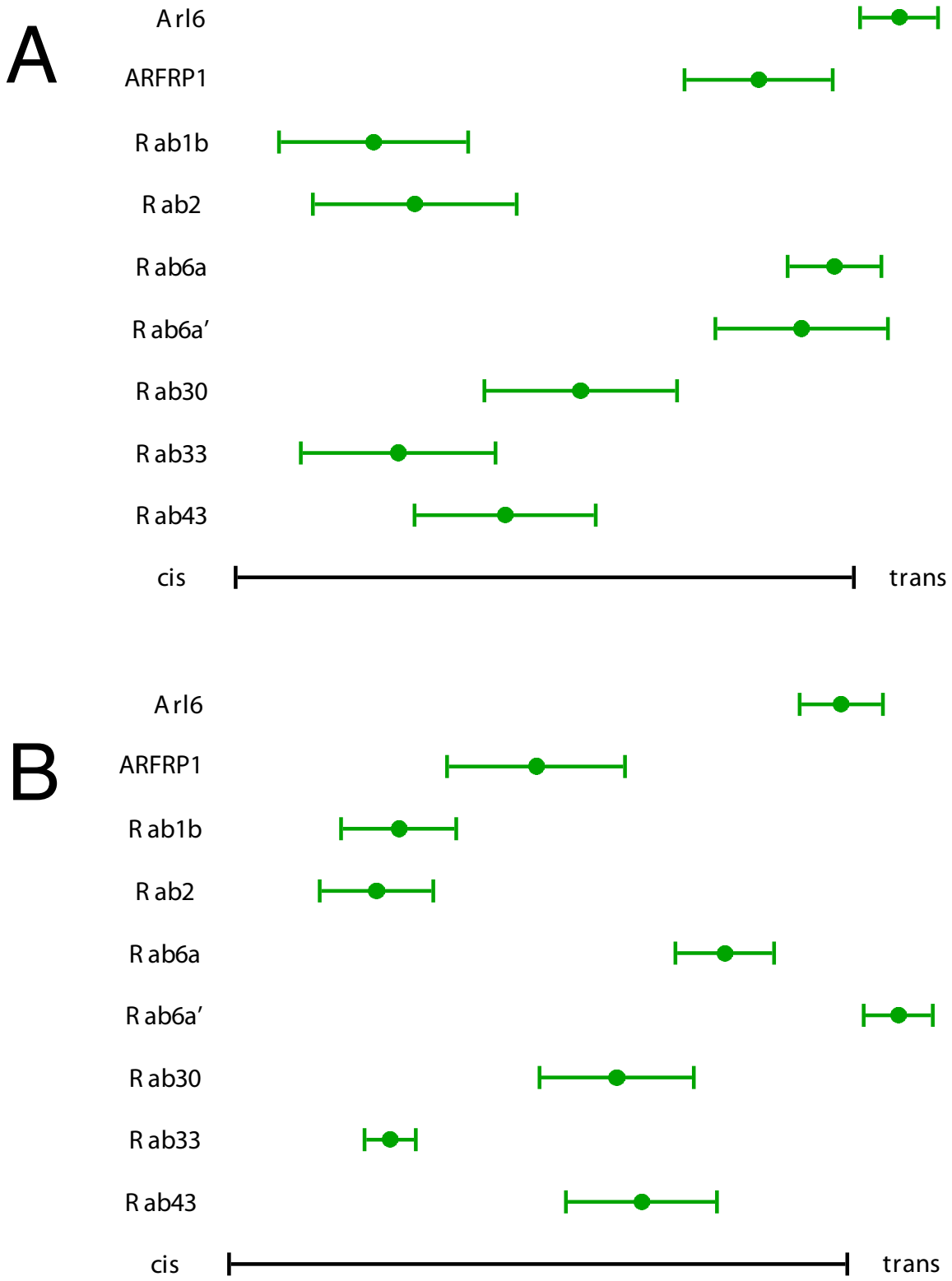

Supplemental Figure 3 Light Microscopic Localization of Rab Proteins to Golgi Subdomains in HeLa Cells. (A) Results of experimental analysis identical to that described in Fig. 2 except that HeLa cells were transfected with the indicated GFP constructs. GM130 was used to mark the cis-Golgi and TGN46 was used to mark the trans-Golgi. The cis-Golgi marker GM130 was visualized using a Cy5-tagged secondary antibody (blue) and the trans-Golgi marker TGN46 was visualized using a Cy3-tagged secondary antibody (red). Values were then rescaled to match the average value of the cis control (an average of Rab1b and Rab2) and the trans control (average of Rab6a and Rab6a') to the values in Fig. 2. (B) Analysis of similarly transfected and stained HeLa cells except that cells were treated with 1 µg/ml nocodazole for 5 hours prior to fixation and predominant Golgi localization was scored using a fully automated procedure as described in Dejgaard et al., (2007). Values were rescaled as described for (A).

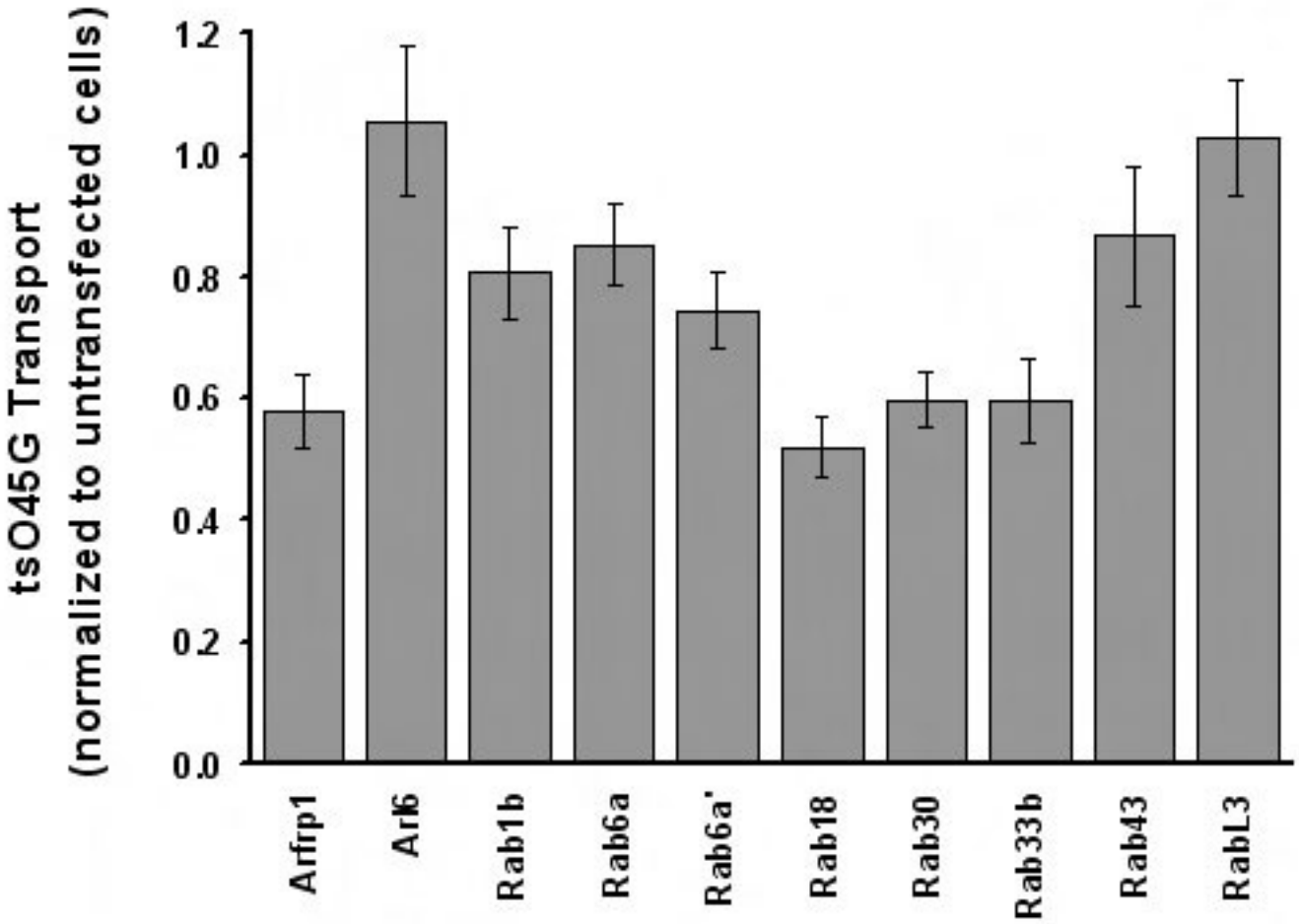

Supplemental Figure 4. Effects of Overexpressed Rab Proteins on Secretion in HeLa Cells. Cell surface arrival of the ts-O45-G mutant of VSVG was measured in cells overexpressing the wild-type Rab proteins, in an automated assay as described previously (Liebel et al., 2003).

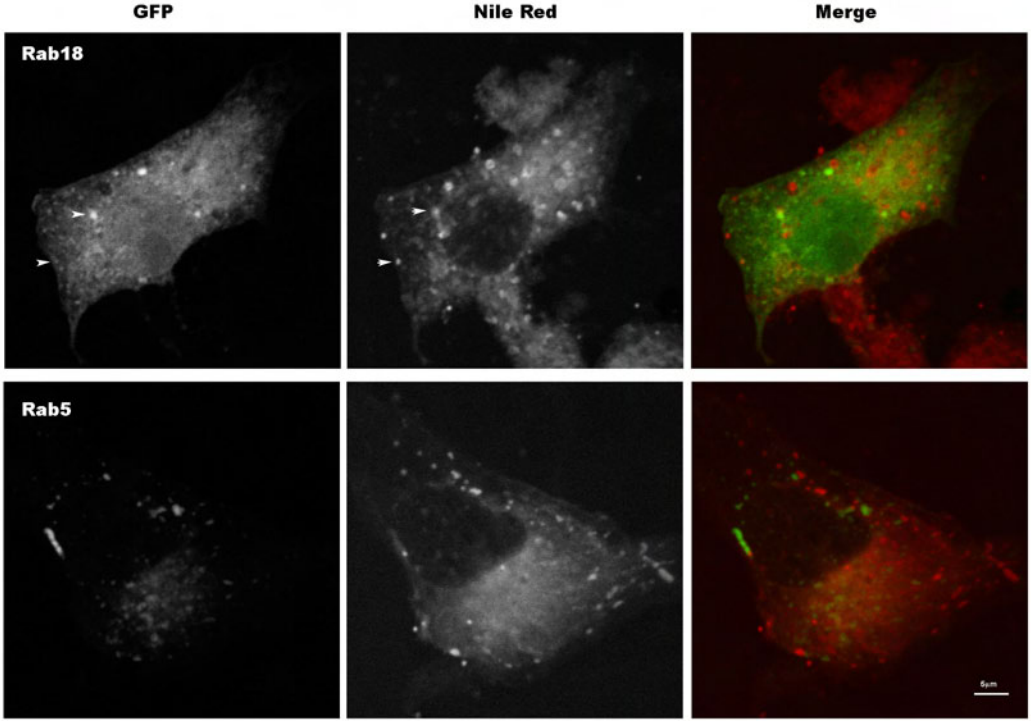

Supplemental Figure 5. Colocalization of Rab18 with Lipid Droplets in Oleic Acid Treated Cells. Vero cells transiently expressing GFP-Rab18 or GFP-Rab5 were incubated with 100 μg/ml oleic acid for 24 hrs. to induce lipid droplet formation as described in Martin et al., (2005) J. Biol. Chem.280:42325-35. Coverslips were then fixed and stained with Nile Red as described in Martin et al. (2005). Images were taken with a Zeiss 510 confocal microscope using a 63x N.A. 1.4 objective. Arrows indicate colocalization. Bar, 5 microns.

Supplemental Table S1: Construction of GFP fusions used in this study[*].		
Protein[**]	Accession Number	Source
Arf2	BC0403661	IRAKp9611E21203Q2
Arf3	BC028402	IRATp970D1028D6
Arf4	BC003364	IRATp970C031D6
Arf5	BC003043	IMAGE:2822973
Arl1	BC007000	IMAGE:3960492
Arl6	BC024239	IMAGE:4826873
Rab1b	AL136635	DKFZp564I172
Rab2a	BC008929	IMAGE:2966694
Rab6b	BC002510	IMAGE:3050592
Rab6c	AL136727	DKFZp566K144
Rab8a	BC002977	IMAGE:3547214
Rab10	BC000896	IMAGE:3464547
Rab14	BC006081	IMAGE:2963119
Rab15	BC040679	IMAGE:4817835
Rab18	AL136734	DKFZp434N0410
Rab24	BC015534	IMAGE:3916832
Rab30	BC014213	IRAUp969A0268D6
Rab33b	AL136904	DKFZp434G099
Rab35	BC015931	IRATp970B1211D
Rab43	BC062319	IMAGE:4873224
RabL3	BC020832	IRAUp969BD388D6
RalA	BC039858	IMAGE:5495399
Rap1b	BC000176	IMAGE:2900837

[*]Human cDNA clones containing the open reading frames of the indicated GTPases were obtained from the RZPD (Berlin, Germany). Rab and Rab-like ORFs were cloned by PCR into the pEGFP/ECFP-C1 vector (BD-Clontech), and Arf and Arf-like ORFs into the pEGFP/ECFP-N1 vector, and all were sequence verified.

[**]Fluorescent tagging of Arf1 (Vasudevan et al., 1998), Rab6a' (Young et al., 2005), Rabs 4, 5, 7, 11 (Hunyady et al., 2002), Rab1a, Rab9a, Rab21, and Rab22a (Simpson et al., 2004), and GFP-p150^{Glued} (Watson and Stephens, 2006) has been described previously.

Supplemental Table S2. Peptides used to identify Ras-family Proteins on the Golgi Complex*

Protein	Accession Number (matched) **	Unique Peptide§	Peptide Unique to Group or Class
Rab1A	763158	NATNVEQSFMTMAAEIK tdacg NATNVEQSFMTMAAEIKK tc VVDYTTAKEFADSLGIPFLETSAK tc VVDYTTAK tcg MGPGATAGGAEK tcg KVVDYTTAK tcg IQSTPVK cg	EFADSLGIPFLETSAK tcg Rab1AB NPEYDYLFK tcg Rab1AB TITSSYYR tcg Rab1AB GAHGIIVVYDVTDQESFNNVK tcg Rab1AB YASENVNK tcg Rab1AB QWLQEIDR tc Rab1AB QWLQEIDRYASENVNK c Rab1AB FADDTYTESYISTIGVDFK tcg Rab1AB SCLLLR cg Rab1AB
Rab1B	226486	EFADSLGVPFLETSAK tdcg GAHGIIVVYDVTDQESYANVK tdcg NATNVEQAFMTMAAEIK tdcg NATNVEQAFMTMAAEIKK c MGPGAASGGERPNLK cg IDSTPVK cg	
Rab2A	13929006	IQEGVFDINNEANGIK tacg DTFNHLTTWLEDAR tdc TASNVEEAFINTAK tdacg RDTFNHLTTWLEDAR t SCLLLQFTDKR t RAB2B	EHGLIFMETSAK tcg RAB2AB LQIWDTAGQESFR tdacg RAB2AB YIIIGDTGVGK tcg Rab2AB KEEGEAFAR cg Rab2AB QHSNSNMVIMLIGNK c Rab2AB
Rab4A	77404180/ 414969	MGSGIQYGDAALR g	
Rab8	131798	ANINVENAFFTLAR tg Rab 8A NIEEHASADVEK tcg Rab8A SSTNVEEAFFTLAR g Rab8B	
Rab10	420269	AFLTLAEDILR tdcg EPNSENVDISSGGGVTGWK g ANINIEK g KTYDLLFK g GAMGIMLVYDITNGK cg AFLTLAEDILR tcg FHTITTSYYR g NIDEHANEDVER tcg	
Rab14	16758368	GAAGALMVYDITR tcg TGENVEDAFLEAAK tdcg TGENVEDAFLEAAKK tdcg NLTNPNTVIILIGNK tcg QFAEENGLLFLEASAK cg LTSEPQPQR g IIEVSGQK g ADLEAQR g IYQNIQDGSLDLNAAESGVQHKPSAPQGGR cg SCLLHQFTEK tcg STYNHLSSWLTDAR g	
Rab15	27666168	IQIWDTAGQER tdac	
Rab35	5803135/ 27666028	LLIIGDSGVGK dc	
Rab43	21746181/	LVLVGDASVGK g	

	14777331	YAGSNIVQLLIGNK td DSSNVEEAFTR td	
Rab5A	12083645	TSMNVNEIFMAIAK tdcg QASPNIVIALSGNK tc GVDLTEPAQPAR tg NEPQNPGANSAR g	YHSLAPMYYR g RAB5ABC LVLLGESAVGK tg RAB5ABC FEIWDTAGQER tcg RAB5ABC
Rab5B	109480137	TAMNVNDLFLAIAK tdcg QASPSIVIALAGNK tdc SEPQNPGGAAGR tg GVDLHEQAQQNK g GAQAAIVVYDITNQETFAR t	
Rab5C	1710027	GVDLQENSPASR td QASPNIVIALAGNK tdacg TAMNVNEIFMAIAK tdcg GVDLQESNPASR tdcg GAQAAIVVYDITNTDTFAR dg NEPQNAAGAPGR cg	
Rab 6A/ 6A'/6B/ 6C	131796 17512290		ELNVMFIETSAK tdacg RAB6AA' QVSIEEGER tdc RAB6AA' QVSIEEGERK d RAB6AA' AKELNVMFIETSAK tdRAB 6AA' TMYLEDR g RAB6AA' SREDMIDIK tcg RAB6AA' LVFLGEQSVGK tdcg RAB6AA'B GSDVIIMLVGNK tdcg RAB6AA'B VAAALPGMESTQDR tdacg RAB6AA'C DSAAAVVVYDITNVNSFQQ TTK t RAB6A'C WIDDVR t RAB6ABC
Rab7	13027392	FQSLGVAFYR tdcg DPENFPFVVLGNK tdacg EAINVEQAFQTIAR tdacg LVTMQIWDTAGQER tdcg TSLMNQYVNK tdcg VIILGDSGVGK tcg DEFLIQASPR g ATIGADFLTK tcg NALKQETEVELYNEFPEPIK g TLDSWRDEFLIQASPR tg NNIPYFETSAK tcg	
RAB9A	16758200	DSTNVAAAFEEAVR dc	FVTLQIWDTAGQER t RAB9AB
Rab11B	14249144	NNLSFIETSALDSTNVEEAFK cg	AQIWDTAGQER tdg RAB11AB GAVGALLVYDIAK tdcg RAB11AB DHADSNIVIMLVGNK cg Rab11AB NEFNLESK cg Rab11AB STIGVEFATR cg Rab11AB VVLIGDSGVGK cg Rab11AB AVPTDEAR cg Rab11AB HLTYENVER cg Rab11AB

			NILTEIYR cg Rab11AB
Rab18	1710017	IIQTPGLWESENQNK tdcg GAQGVILVYDVTR tdcg TCDGVQCAFEELVEK tdcg NDIVNMLVGNK dcg ILIIGESGVGK dcg FTDDTFDPELAATIGVDFK tc LDNWLNELETYCTR g HSMLFIEASAK g NDIVNMLVGNKIDK c	
Rab21	576556	HVSIQEAESYAESVGAK c MIETAQVDER g HITTLQASFLTK t	
Rab22A	631514	NAININELFIEISR dg	FLIWDTAGQER g Rab22AB
Rab30	62543511	QNTLVNNVSSPLPGEGK c VITVLVGNK c	
Rab33B	2516239	IQLWDTAGQER tdac NPNDNDHVEAIFMTLAHK td SAIQVPTDLAQK tdac SHKPLMLSQLPDNR td FADTHSMPLFETSAK d	TEATIGVDFR d RAB33AB
RabL3	109494358	EQFADNQIPLLVIGTK g VLVLGDSGVGK cg	
RalA	131836	ADQWNVNYVETSAK t	
ARF1	4502201		QDLPNAMNAAEITDK g ARF1-ARF3 MLAEDELR g ARF1-ARF3 LGLHSLR g ARF1-ARF3 NISFTVWDVGGQDK g ARF1-ARF3
ARF2	51316991		
ARF3	20306322		
ARF4	13097192	MLLEDELQDAVLLLFANK g LGLQSLR g QDLPNAMAISEMTDK g IQEGAAVLQK g	NICFTVWDVGGQDK g ARF4, ARF5
ARF5	2137130	VQESADELQK tdg QDMPNAMPVSELTDK g LGLQHLR g MLQEDELR g	
ARF6	13162345	HYYTGTQGLIFVVDCADR g ARF6 LGQSVTTIPTVGFNVETVTYK g ARF6 ILMLGLDAAGK g ARF6	
ARF1-6 pool		DAVLLVFANK tg ARF1, ARF3, ARF5 HYFQNTQGLIFVVDSNDR g ARF1-ARF5 HYFQNTQGLIFVVDSNDRER g ARF1-ARF5 LGEIVTTIPTIGFNVETVEYK g ARF1-ARF5 ILMVGLDAAGK g ARF1-ARF5 TTILYK g ARF1-ARF5, ARF6, ARL14h (ARF7)	
ARD1	543840	DALLLIFANK g	
ARFRP1 or ARP1	7012932	VVSSEALDGVPILVLANK tdcg DCLTQACSALTGK tdcg ITTTVGLNIGTVDVGK tdacg QDVETCLSIPDIK c TTFLEQSK c YTLLSGLYK g	
ARL1	728888	SELVAMLEEEELRK tdcg GTGLDEAMEWLVETLK tdg	

		SELVAMLEEEELR g ILILGLDGAGK tg LQVGEVVTTIPTIGFNVETVTYK g	
ARL6IP2	10439926/ 62650248	SMLQATAEANNLAAVAGAR t NLVPLLLAPENLVEK g LAMEEIYQKPFQTLMFLIR t NLVPLLLAPENLVEK tg	IYQGEELPHPK t atlastin isoform b, Spg3, ARL6IP2
Cdc42	887408/ 385323	NVFDEAILAALEPPEPK td TPFLLVGTQIDLR d	
Galphai2	13591955		IAQSDYIPTQQDVLR c Gnai1 Gnai2
RHOA	16923986		TCLLIVFSK c RhoA, RhoB, RhoC, RHO H6, RHO H12, RSA-14-44 protein
Rap1B	595280	VKDTDDVPMILVGNK td	INVNEIFYDLVR td Rap1AB
PRA1	2564205	DAEVEGLSATTLLPK td ATIRPWGTFVDQQR td	
SAR1A	548898	NYLPAINGIVFLVDCADHSR g EIFGLYGQTTGK g VELNALMTDETISNVPILILGNK g	LVFLGLDNAGK dg Sar1AB QGYGEGFR g Sar1AB

* Since the number of Ras-family proteins of interest was small relative to the total Golgi complement of proteins, we manually screened by BLAST peptides identified by MASCOT from each of the five rat liver Golgi preparations examined in (Gilchrist et al., 2006; total Golgi, detergent fraction, aqueous fraction, and COPI vesicles prepared with GTP or GTPγS). Since annotation of the Rattus norvegicus database was still in progress, both MASCOT and BLAST were run separately against Rattus norvegicus, Mus musculus and Homo sapiens databases. Uniqueness/sharing of peptides was checked using a Ruby script which produced as output for each peptide a protein or list of proteins sharing that peptide.

**Protein accession number are given for human, rat, mouse, or dog.

§Fraction: t, total; d, detergent; a, aqueous; c, COPI vesicles (GTP); g, COPI vesicles (GTPγS)

Table S3. GFP-tagged constructs used in this study.

Protein	Accession Number *	Localization (this study)†	Published Location	Mutation Tested††
Arf1	4502201	Golgi	Golgi [1, 2]	T31N, Q71L
Arf2	51316982[r]	Golgi	Golgi [3]	T31N, Q71L
Arf3	20306322	Golgi	Golgi [3, 4]	T31N, Q71L
Arf4	13097192	Golgi	Golgi [5]	T31N, Q71L
Arf5	12804365	Golgi	Golgi [3, 4]	T31N, Q71L
ARFRP1	14715092[m]	Golgi	Golgi [6-8]	T31N, Q79L
Arl1	13937801	Diffuse	Golgi [9]	T31N, Q71L
Arl6	18999390	Golgi + ER	Cytosol [10]	T31N
Rab1a	14705268	Golgi + ER	Golgi + ER [11]	S25N
Rab1b	13569962	Golgi + ER	Golgi + ER [12]	S22N
Rab2a	33869422	Golgi + ER	Golgi + ER [11]	S20N
Rab4b	919	Endosome (some Golgi)	Endosome [13]	S22N
Rab5a	164056[c]	Endosome (some Golgi)	Endosome [11]	S34N
Rab6a	550072**	Golgi	Golgi [14]	T27N
Rab6a'	8163754	Golgi	Golgi [15]	T27N
Rab6b	12803379	Golgi	Golgi [16]	T27N
Rab6c	12052973	Punctate†††	Cytosol [17]	T27N
Rab7	164058[c]	Endosome	Endosome [11]	N125I
Rab8	12804237	ER + punctae	Cell surface [18] Post-Golgi vesicles [19]	T22N
Rab9a	2190[c]	Golgi + endosome	Golgi + endosomes [20]	S21N
Rab10	12654157	Diffuse	Golgi [18] Endosomes [21]	T23N
Rab11	917[c]	Endosome	Endosomes [22]	S25N
Rab14	13543869	Golgi + punctae	TGN, endosomes [23]	S25N
Rab15	34783347	Nucleus	Endosome [24]	T22N
Rab18	12052987	ER, Golgi (some cell types)	Endosome [25, 26] Lipid droplet [27]	S22N, Q67L
Rab21	7661922	Endosome	Endosome [28]	T33N, Q78L
Rab22a	16041684	Endosome	Endosome [29]	S19N
Rab24	15930203	ER†††	ER [29]	T21N
Rab30	15559714	Golgi + ER	Golgi [30]	T23N, Q68L
Rab33b	12053305	Golgi	Golgi [31, 32]	S42N
Rab35	16198501	Cell surface, Endosomes	Endosomes [33]	S22N, Q67L
Rab43	38382891	Golgi + ER	Golgi [34]	T32N
RabL3	18088572	Cytosol + Actin	n.d.	S20N
RalA	24980847	Filopodia	Filipodia [35]	S28N, Q72L
Rap1b	12652847	Cytosol	Endosomes [36]	S 17N
Cdc42	4757952	Golgi (weak)	Golgi [37]	T17N
RhoA	62896671	Cytosol	Cytosol [37]	T19N

* Protein accession numbers of tagged cDNA's are human unless otherwise indicated ([c] Canis familaris; [m] Mus musculis; [r] Rattus norvegicus). All proteins were tagged with EGFP on the N-terminus except Arf1, Arf5, ARFRP1, Arl1 and Arl6 were tagged on the C-terminus. We chose for GFP-tagging any Ras-family protein identified by unique peptides (excluding Sar1 as not likely to have a function on Golgi membranes) except that out of some groups of highly homologous proteins we chose one or more representatives.

** Rab6a was made from Rab6a' by site-directed mutagenesis. Final protein sequence is that found in gi|550072.

† Most constructs showed considerable non-localized cytosolic labeling. This is not indicated unless no other localization was found.
††Dominant-negative and positive mutants were made by site-directed mutagenesis using the Stratagene QuickChange strategy (Stratagene, La Jolla, CA) and then sequence verified. GFP-Rab6a was made from GFP-Rab6a' by site directed mutagenesis.
††† Rab6c and Rab24 were not identified by unique peptides. They were GFP-tagged as controls.

1. Stearns, T., Willingham, M. C., Botstein, D. & Kahn, R. A. ADP-ribosylation factor is functionally and physically associated with the Golgi complex. Proc. Natl. Acad. Sci. U. S. A. 87, 1238-42 (1990).
2. Teal, S. B., Hsu, V. W., Peters, P. J., Klausner, R. D. & Donaldson, J. G. An activating mutation in ARF1 stabilizes coatomer binding to Golgi membranes. J. Biol. Chem. 269, 3135-8 (1994).
3. Hosaka, M. et al. Structure and intracellular localization of mouse ADP-ribosylation factors type 1 to type 6 (ARF1 -- ARF6). J. Biochem. 120, 813-9 (1996).
4. Tsai, S.-C., Adamik, R., Haun, R. S., Moss, J. & Vaughan, M. Differential interaction of ADP-ribosylation factors 1, 3 and 5 with rat brain Golgi membranes. Proc. Natl. Acad. Sci. U. S. A. 89, 9272-6 (1992).
5. Deretic, D. et al. Rhodopsin C terminus, the site of mutations causing retinal disease, regulates trafficking by binding to ADP-ribosylation factor 4 (ARF4). Proc. Natl. Acad. Sci. U. S. A. 102, 3301-6 (2005).
6. Behnia, R., Panic, B., Whyte, J. R. C. & Munro, S. Targeting of the Arf-like GTPase Arl3p to the Golgi requires N-terminal acetylation and the membrane protein Sys1p. Nature Cell Biol. 6, 405-13 (2004).
7. Shin, H.-W. et al. Roles of ARFRP1 (ADP-ribosylation factor-related protein 1) in post-Golgi membrane trafficking. J. Cell Sci. 118, 4039-48 (2005).
8. Zahn, C. et al. Knockout of Arfrp1 leads to disruption of ARF-like1 (ARL1) targeting to the trans-Golgi in mouse embryos and HeLa cells. Mol. Membr. Biol. 23, 475-85 (2006).
9. Lowe, S. L., Wong, S. H. & Hong, W. The mammalian ARF-like protein 1 (Arl1) is associated with the Golgi complex. J. Cell Sci. 109, 209-220 (1996).
10. Ingley, E. et al. A novel ADP-ribosylation like factor (ARL-6) interacts with the protein-conducting channel SEC61beta subunit. FEBS Lett. 459, 69-74 (1999).
11. Chavrier, P., Parton, R. G., Hauri, H.-P., Simons, K. & Zerial, M. Localization of low molecular weight GTP binding proteins to exocytic and endocytic compartments. Cell 62, 317-29 (1990).
12. Plutner, H. et al. Rab1b regulates vesicular transport between the endoplasmic reticulum and successive Golgi compartments. J. Cell Biol. 115, 31-43 (1991).
13. Van Der Sluijs, P. et al. The small GTP-binding protein rab4 is associated with early endosomes. Proc. Natl. Acad. Sci. U. S. A. 88, 6313-7 (1991).
14. Goud, B., Zahraoui, A., Tavitian , A. & Saraste, J. Small GTP-binding protein associated with Golgi cisternae. Nature 345, 553-6 (1990).
15. Mallard, F. et al. Early/recycling endosomes-to-TGN transport involves two SNARE complexes and a Rab6 isoform. J. Cell Biol. 156, 653-64 (2002).
16. Opdam, F. J. M. et al. The small GTPase Rab6B, a novel Rab6 subfamily member, is cell-type specifically expressed and localised to the Golgi apparatus. J. Cell Sci. 113, 2725-35 (2000).
17. Tian, K., Jurukovski, V., Yuan, L., Shan, J. & Xu, H. WTH3, which encodes a small G protein, is differentially regulated in multidrug-resistant and sensitive MCF7 cells. Cancer. Res. 65, 7421-8 (2005).
18. Chen, Y.-T., Holcomb, C. & Moore, H. P. H. Expression and localization of two low molecular weight GTP-binding proteins, Rab8 and Rab10 by epitope tag. Proc. Natl. Acad. Sci. U. S. A. 90, 6508-12 (1993).
19. Huber, L. A. et al. Rab8, a small GTPase involved in vesicular traffic between the TGN and the basolateral plasma membrane. J. Cell Biol. 123, 35-45 (1993).
20. Lombardi, D. et al. Rab9 functions in transport between late endosomes and the trans Golgi network. EMBO J. 12, 677-82 (1993).
21. Babbey, C. M. et al. Rab10 regulates membrane transport through early endosomes of polarized Madin-Darby canine kidney cells. Mol. Biol. Cell 17, 3156-75 (2006).
22. Ullrich, O., Reinsch, S., Urbe, S., Zerial, M. & Parton, R. G. Rab11 regulates recycling through the pericentriolar recycling endosome. J. Cell Biol. 135, 913-24 (1996).

23. Junutula, J. R. et al. Rab14 is involved in membrane trafficking between the Golgi complex and endosomes. Mol. Biol. Cell 15, 2218-29 (2004).
24. Zuk, P. A. & Elferink, L. A. Rab15 mediates an early endocytic event in Chinese hamster ovary cells. J. Biol. Chem. 274, 22303-12 (1999).
25. Lutcke, A. et al. Cloning and subcellular localization of novel rab proteins reveals polarized and cell type-specific expression. J. Cell Sci. 107, 3437-48 (1994).
26. Yu, H., Leaf, D. S. & Moore, H. P. H. Gene cloning and characterization of a GTP-binding Rab protein from mouse pituitary AtT-20 cells. Gene 132, 273-8 (1993).
27. Martin, S., Driessen, K., Nixon, S. J., Zerial, M. & Parton, R. G. Regulated localization of Rab18 to lipid droplets. J. Biol. Chem. 280, 42325-35 (2005).
28. Simpson, J. C. et al. A role for the small GTPase Rab21 in the early endocytic pathway. J. Cell Sci. 117, 6297-311 (2004).
29. Olkkonen, V. M. et al. Molecular cloning and subcellular localization of three GTP-binding proteins of the rab subfamily. J. Cell Sci. 106, 1249-61 (1993).
30. de Leeuw, H. P. et al. Small GTP-binding proteins in human epithelial cells. Brit. J. Haem. 103, 15-9 (1998).
31. Valsdottir, R. et al. Identification of rabaptin-5, rabex-5, and GM130 as putative effectors of rab33b, a regulator of retrograde traffic between the Golgi apparatus and ER. FEBS Lett. 508, 201-9 (2001).
32. Zheng, J. Y. et al. A novel Rab GTPase, Rab33B, is ubiquitously expressed and localized to the medial Golgi cisternae. J. Cell Sci. 111, 1061-9 (1998).
33. Kouranti, I., Sachse, M., Arouche, N., Goud, B. & Echard, A. Rab35 regulates an endocytic recycling pathway essential for the terminal steps of cytokinesis. Curr. Biol. 16, 1719-25 (2006).
34. Haas, A. K., Fuchs, E., Kopajtich, R. & Barr, F. A. A GTPase-activating protein controls Rab5 function in endocytic trafficking. Nature Cell Biol. 7, 887-93 (2005).
35. Ohta, Y., Suzuki, N., Nakamura, S., Hartwig, J. H. & Stossel, T. P. The small GTPase RalA targets filamin to induce filopodia. Proc. Natl. Acad. Sci. U. S. A. 96, 2122-8 (1999).
36. Pizon, V., Desjardins, M., Bucci, C., Parton, R. G. & Zerial, M. Association of Rap1a and Rap1b proteins with late endocytic/phagocytic compartments and Rab2a with the Golgi complex. J. Cell Sci. 107, 1661-70 (1994).
37. Michaelson, D. et al. Differential localization of Rho GTPases in live cells: regulation by hypervariable regions and RhoGDI binding. J. Cell Biol. 152, 111-26 (2001).